Probabilistic Engineering Mechanics 66 (2021) 103157

Contents lists available at ScienceDirect

Probabilistic Engineering Mechanics

journal homepage: www.elsevier.com/locate/probengmech

Neumann enriched polynomial chaos approach for stochastic finite element problems

S.E. Pryse, S. Adhikari *

College of Engineering, Swansea University, Swansea, UK

ARTICLE INFO

Keywords:
Polynomial chaos expansion
Neumann expansion
Model reduction
Uncertainty quantification
Enrichment

ABSTRACT

An enrichment scheme based upon the Neumann expansion method is proposed to augment the deterministic coefficient vectors associated with the polynomial chaos expansion method. The proposed approach relies upon a split of the random variables into two statistically independent sets. The principal variability of the system is captured by propagating a limited number of random variables through a low-ordered polynomial chaos expansion method. The remaining random variables are propagated by a Neumann expansion method. In turn, the random variables associated with the Neumann expansion method are utilised to enrich the polynomial chaos approach. The effect of this enrichment is explicitly captured in a new augmented definition of the coefficients of the polynomial chaos expansion. This approach allows one to consider a larger number of random variables within the scope of spectral stochastic finite element analysis in a computationally efficient manner. Closed-form expressions for the first two response moments are provided. The proposed enrichment method is used to analyse two numerical examples: the bending of a cantilever beam and the flow through porous media. Both systems contain distributed stochastic properties. The results are compared with those obtained using direct Monte Carlo simulations and using the classical polynomial chaos expansion approach.

1. Introduction

System and structural uncertainties may result in considerable differences arising in the responses of seemingly equivalent systems. Such uncertainties can occur in numerous ways including during the manufacturing or assembly processes of a structure, or in an applied load. Consequently, methods for quantifying and analysing stochastically parametrised systems have been developed. Through the use of such efficient numerical algorithms, systems that are governed by stochastic partial differential equations can be efficiently analysed.

Due to its rigour and efficient manner, the stochastic finite element approach has been widely utilised to model and propagate uncertainty. Through this approach, one or more distributed parameters can be modelled by random fields. In the context of elliptic problems, the governing equation can be expressed as

$$-\nabla^n \left[a(x,\theta)\nabla^n u(x,\theta)\right] = p(x); \quad x \text{ in } \mathscr{D} \tag{1}$$

with the Dirichlet boundary condition $u(x,\theta) = 0$, x on $\partial\mathscr{D}$. The spacial domain under consideration is defined as $\mathscr{D} \in \mathbb{R}^d$ with piecewise Lipschitz boundary $\partial\mathscr{D}$, and d is less than or equal to 3. In the above equation, x is the spatial variable, θ denotes sample space, $p(x)$ is the excitation, $u(x,\theta)$ is the response of the system and $a(x,\theta)$ is the random field describing a system parameter. The random field is on a bounded domain on $\mathbb{R}^d$ and on the probability space $(\Theta, \mathcal{F}, P)$. The differential operator is given by ∇, whilst the value of n is problem dependent. To solve the stochastic partial differential equation given in Eq. (1), it is necessary to discretise both the response and the random field. The response field can be discretised by utilising the conventional finite element method, while the stochastic field can be discretised, in our case, through the Karhunen–Loève expansion

$$a(x,\theta) = a_0(x) + \sum_{i=1}^{\infty} \sqrt{\nu_i}\xi_i(\theta)\varphi_i(x) \tag{2}$$

In the above expression $a_0(x)$ is the mean function, $\xi_i(\theta)$ are uncorrelated standard Gaussian random variables. ν_i and $\varphi_i(x)$ correspond to the eigenvalues and eigenfunctions of the autocorrelation function of the random field. Substituting the Karhunen–Loève expansion into Eq. (1) and truncating the series up to Mth term, the discretised equation can be expressed as

$$\left[\mathbf{A}_0 + \sum_{i=1}^{M} \xi_i(\theta)\mathbf{A}_i\right]\mathbf{u}(\theta) = \mathbf{f} \tag{3}$$

The response vector $\mathbf{u}(\theta)$ may be obtained by directly solving the above equation through the use of a direct Monte Carlo method. However the convergence rate of the method is notoriously slow, hence a large number of computationally expensive simulations is required. In order to overcome the computational cost, a number of efficient techniques

* Corresponding author.
E-mail address: S.Adhikari@swansea.ac.uk (S. Adhikari).

https://doi.org/10.1016/j.probengmech.2021.103157
Received 31 March 2020; Received in revised form 26 April 2021; Accepted 12 July 2021
Available online 19 July 2021

have been proposed to approximate the response of structural systems. One such method is the Polynomial Chaos Expansion [PCE]. The PCE method was first discussed by Wiener in his 1938 work [1]. This work utilised both Hermite polynomials and Gaussian random variables to describe a stochastic process. The first application of the PCE method in conjunction with the stochastic finite element method was conducted and was entitled the Spectral Stochastic Finite Element Method. The first application of the PCE method to analyse engineering systems was conducted by Gahnem and Spanons [2], and the proposed framework was entitled the Spectral Stochastic Finite Element Method. Following this, the PCE method has been widely applied in numerous fields including structural dynamics [3,4], heat transfer [5,6] and fluid dynamics [7,8]. The method has also been utilised to analyse systems undergoing static loads [9] and dynamic loads in both the time [10] and frequency [11,12] domains. In addition to analysing the responses of stochastically parametrised systems, the PCE method has also been applied to the random eigenvalue problem [13,14]. In turn, methods which hybridise the perturbation method and the PCE have been suggested to analyse the random eigenvalue problem [15]. These hybridised methods have been obtained by utilising a collection of methods including the Rayleigh quotient, the power method and the inverse power method.

One of the main necessities of the PCE method is to determine the deterministic PCE coefficients. The methods for obtaining these deterministic coefficients can be categorised into two groups, intrusive or non-intrusive methods [16]. The intrusive method corresponds to the method discussed above. This method ensures that the residual of stochastic finite element formulation is orthogonal to the basis associated with the PCE method. Non-intrusive methods are often treated as black box solvers where a number of samples are treated deterministically. Extensive literature have discussed different non-intrusive methods. These approaches include projection methods [17,18], least squares approximations [19,20], stochastic collocation methods [21,22] and efficient sampling methods such as Latin hypercube or quasi sampling methods [23,24]. Numerous studies have been conducted to compare different non-intrusive methods [25–28]. In one such study, the effect of altering the number of sample points for non-intrusive PCE methods was systematically examined [28]. The work concluded that in order to have an accurate account of a stochastic system, the number of sample points is required to be at least twice the number of terms in PCE.

One of the main restrictions associated with the PCE is the large computational cost associated with high dimensional systems. The number of terms associated with the PCE increases exponentially with the dimension of the stochastically parametrised system. In order to address this issue, sparse representations of the PCE have been suggested [29–33]. Such methods are achieved by only retaining the dominant basis functions which are associated with the PCE method. It has also been demonstrated that the convergence of the statistical moments can be very slow for dynamic problems. In order to address this, a method for accelerating the convergence of the first two statistical moments has been suggested [4]. Furthermore, the PCE is reported to produce erroneous peaks at resonance frequencies [4]. This is of importance as the resonance values have physical interpretation. For a comprehensive discussion about the limitations, see [34–36].

One of the most pressing issues associated with the PCE is its vulnerability to the curse of dimensionality when the number of stochastic dimensions is large. In numerous studies, the number of stochastic dimensions is often truncated. This can lead to valuable information being omitted from the solution. As a result, this work aims to address this issue by exploring a hybrid enrichment method. A limited number of hybrid methods have been suggested in conjunction with the PCE. Among the hybrid techniques, the Kriging method [37] has recently been utilised to produce a new non-intrusive meta-modelling method [38,39]. In these studies, a system's global behaviour is modelled by the PCE, and the local behaviour by the Kriging method. The Arnoldi-based Krylov subspace technique [40] has also been used in conjunction with the PCE method [41]. The work applies the Arnoldi-based Krylov subspace technique to reduce the size of the governing stochastic finite element equation prior to utilising the PCE method. In our proposed method, a hybridised Neumann enrichment approach is proposed to enrich the PCE method. This is achieved by initially propagating a limited number of random variables through the PCE method. The remaining random variables are utilised to enrich the PCE coefficients by the use of a Neumann series expansion.

The paper is structured as follows. An overview of the well-established polynomial chaos expansion is given in Section 2. In a similar manner, Section 3 outlines the Neumann Expansion method. Section 4 introduces the novel enrichment approach. Closed-form expression for both the mean and the variance of the classical polynomial chaos expansion method and the Neumann enriched polynomial chaos expansion method are discussed and provided in Section 5. Section 6 utilises the Neumann enriched polynomial chaos expansion method to approximate the response of a Euler–Bernoulli cantilever beam and a flow through a porous media. Both systems contain stochastic properties. These results are compared with the benchmark direct Monte Carlo simulation approach and the classical polynomial chaos method. The major findings and conclusions are consequently drawn in Section 7.

2. Polynomial chaos expansion

Let $\boldsymbol{\xi}(\theta) = \{\xi_1(\theta), \xi_2(\theta), \dots, \xi_M(\theta)\}$ be a set of M independent and identically distributed input random vectors that represent the input uncertainty of a system (here θ denotes the sample space). By applying the PCE approach, the stochastic response $u_j(\theta)$ can be represented with a mean-square convergent series as

$$\begin{aligned} u_j(\theta) = u_{i_0}^{(j)} h_0 &+ \sum_{i_1=1}^{\infty} u_{i_1} h_1(\xi_{i_1}(\theta)) \\ &+ \sum_{i_1=1}^{\infty} \sum_{i_2=1}^{i_1} u_{i_1,i_2}^{(j)} h_1(\xi_{i_1}(\theta), \xi_{i_2}(\theta)) \\ &+ \sum_{i_1=1}^{\infty} \sum_{i_2=1}^{i_1} \sum_{i_3=1}^{i_2} u_{i_1,i_2,i_3}^{(j)} h_1(\xi_{i_1}(\theta), \xi_{i_2}(\theta), \xi_{i_3}(\theta)) \\ &+ \sum_{i_1=1}^{\infty} \sum_{i_2=1}^{i_1} \sum_{i_3=1}^{i_2} \sum_{i_4=1}^{i_3} u_{i_1,i_2,i_3,i_4}^{(j)} h_1(\xi_{i_1}(\theta), \xi_{i_2}(\theta), \xi_{i_3}(\theta), \xi_{i_4}(\theta)) + \cdots \end{aligned} \tag{4}$$

where $u_{i_1,\dots,i_p}^{(j)}$ and $u_{i_0}^{(j)}$ are deterministic constants to be determined and $h_p(\xi_{i_1}(\theta), \dots, \xi_{i_p}(\theta))$ is the pth order chaos term. The accuracy of the approximation can be controlled by the order of the chaos terms. The higher the order, the more accurate the approximation. When utilising Gaussian random variables the chaos terms correspond to Hermite polynomial, where the Hermite polynomial are orthogonal with respect to the Gaussian joint distribution function. Due to the response of Eq. (3) being a vector, the scalars $u_{i_1,\dots,i_p}^{(j)}$ and $u_{i_0}^{(j)}$ can be replaced by the vectors $\mathbf{u}_{i_1,\dots,i_p}^{(j)} \in \mathbb{R}^N$ and $\mathbf{u}_{i_0}^{(j)} \in \mathbb{R}^N$. After a finite truncation, the polynomial chaos expansion can be written as

$$\mathbf{u}(\theta) = \sum_{k=1}^{P} H_k(\boldsymbol{\xi}(\theta)) \mathbf{u}_k \tag{5}$$

where $H_k(\boldsymbol{\xi}(\theta))$ are the polynomial chaoses and $\mathbf{u}_k$ are deterministic vectors that need to be determined. The expression for the polynomial chaoses of order p is given by

$$H_k(\boldsymbol{\xi}(\theta)) = (-1)^p \frac{\partial^p}{\partial \xi_{i_1} \dots \partial \xi_{i_p}} \exp^{-\frac{1}{2}\boldsymbol{\xi}^T(\theta)\boldsymbol{\xi}(\theta)} \tag{6}$$

Although this work focuses on the Gaussian distribution, other non-Gaussian random distributions can be considered through the use of a Wiener–Askey polynomial chaos expansion [42,43]. This approach

Table 1
Types of Wiener–Askey polynomial chaoses and their corresponding random input variables.

Random input	Wiener–Askey chaos	Support
Beta	Jacobi	[a, b]
Gamma	Laguerre	[0, ∞]
Gaussian	Hermite	(−∞, ∞)
Uniform	Legendre	[a, b]

Table 2
The value of P when $M = \{2, 3, 5, 10, 20, 50, 100\}$ and $p = \{1, 2, 3\}$.

$Value of M$	2	3	5	10	20	50	100
1st order PC	3	4	6	11	21	51	101
2nd order PC	6	10	21	66	231	1326	5151
3rd order PC	10	20	56	286	1771	23426	176851

provides generalised functional basis where the basis ensure that orthogonality with respect to the probability density functions is kept. Different types of Wiener–Askey polynomial chaoses and their corresponding random variables and supports are provided in Table 1. The value of P arising in Eq. (5) is determined by a basic random variable M and by the order of the PCE (p). In this instance, M corresponds to the order of the Karhunen–Loève expansion

$$P = \sum_{j=0}^{p} \frac{(M+j-1)!}{j!(M-1)!} = \binom{M+p}{p} \tag{7}$$

It is evident that P increases rapidly when either the order of the Karhunen–Loève expansion or the order of the Polynomial Chaos expansion is increased. This is illustrated in Table 2.

The unknown deterministic vectors $\mathbf{u}_k$ can be obtained by utilising a Galerkin error minimising approach [2]. This approach is initiated by substituting the approximation for $\mathbf{u}(\theta)$, which is given by Eq. (5), into the governing discretised model. The residual of the discretised system is subsequently made orthogonal to the space spanned by the polynomial chaoses. In turn, this leads to a system of linear equations of size $NP \times NP$, where N corresponds to the number of degrees of freedom associated with a structure

$$\begin{bmatrix} \widetilde{A}_{1,1} & \cdots & \widetilde{A}_{1,NP} \\ \widetilde{A}_{2,1} & \cdots & \widetilde{A}_{2,NP} \\ \vdots & \vdots & \vdots \\ \widetilde{A}_{NP,1} & \cdots & \widetilde{A}_{NP,NP} \end{bmatrix} \begin{Bmatrix} \widetilde{u}_1 \\ \widetilde{u}_2 \\ \vdots \\ \widetilde{u}_{NP} \end{Bmatrix} = \begin{Bmatrix} \widetilde{f}_1 \\ \widetilde{f}_2 \\ \vdots \\ \widetilde{f}_{NP} \end{Bmatrix} \tag{8}$$

or

$$\widetilde{\mathbf{A}}\mathbf{U}_0 = \mathbf{F} \tag{9}$$

By correctly arranging the linear equations, it can be deduced that

$$\mathbf{U}_0 = \{\mathbf{u}_1^T, \mathbf{u}_2^T, \ldots, \mathbf{u}_P^T\}^T \tag{10}$$

One of the major drawbacks associated with the PCE approach is the high computational cost associated with computing the deterministic vectors $\mathbf{u}_k$. As the value of P increases exponentially with M, this work aims to produce a reduced method which would incorporate a limited number of random variables within the polynomial chaos expansion.

3. Neumann expansion method

Following the application of the stochastic finite element method, the response vector $\mathbf{u}(\theta)$ can be obtained by inverting the system matrix. However, due to the high computational cost associated with inverting the system matrix, a Neumann expansion can be utilised to approximate the inversion. In turn, an approximation for the response vector can be computed. Eq. (3) can be expressed as

$$\mathbf{A}_0 \left[\mathbf{I} + \mathbf{A}_0^{-1} \sum_{i=1}^{\infty} \mathbf{A}_i \xi_i(\theta)\right] \mathbf{u}(\theta) = \mathbf{f}_0 \tag{11}$$

where $\mathbf{A}_0$ is the deterministic contribution of the system matrix, and $\mathbf{I}$ is a $N \times N$ identity matrix. By manipulating the above equation, the response vector can take the following form

$$\mathbf{u}(\theta) = \left[\mathbf{I} + \mathbf{A}_0^{-1} \sum_{i=1}^{\infty} \mathbf{A}_i \xi_i(\theta)\right]^{-1} \mathbf{u}_0 \tag{12}$$

where

$$\mathbf{u}_0 = \mathbf{A}_0^{-1} \mathbf{f}_0 \tag{13}$$

If the inverse of the system matrix exists, the inverse observed in Eq. (12) can by expanded by a convergent series. Thus by applying the Neumann series expansion, Eq. (12) can be expressed as

$$\mathbf{u}(\theta) = \sum_{k=0}^{\infty} (-1)^k \left[\mathbf{A}_0^{-1} \sum_{i=1}^{\infty} \mathbf{A}_i \xi_i(\theta)\right]^k \mathbf{u}_0 \tag{14}$$

where the first three terms of the Neumann series expansion are given by

$$\mathbf{u}(\theta) = \left[\mathbf{I} - \mathbf{A}_0^{-1} \sum_{i=1}^{\infty} \mathbf{A}_i \xi_i(\theta) + \left(\mathbf{A}_0^{-1} \sum_{i=1}^{\infty} \mathbf{A}_i \xi_i(\theta)\right)^2 - \cdots\right] \mathbf{u}_0 \tag{15}$$

By applying suitable truncations to the Karhunen–Loève expansion and the order of the Neumann series expansion, a closed form expression for the response vector can be obtained. One of the main limitations associated with the Neumann expansion method is that the coefficient of variation associated with the stochastic system must not exceed 20%. Furthermore, the spectral radius of the result of $\mathbf{A}_0^{-1} \sum_{i=0}^{\infty} \mathbf{A}_i \xi_i(\theta)$ must be smaller than 1 to ensure the convergence of the Neumann series expansion.

4. Neumann enriched polynomial chaos expansion

4.1. Partitioning the stochastic space

The exponentially increasing cost is one of the main limitations associated with the PCE method. As a result, the values of M and p must be kept relatively low in order for the PCE method to be computationally feasible. This is especially true if the number of degrees of freedom is large. However, by limiting the value of either M or p, valuable information concerning the stochastic properties of the structural system is lost. Therefore, this section aims to suggest a new hybrid method which enriches a low-ordered PCE representation with a Neumann expansion. The crux of the proposed method is to propagate a limited number of random variables through a low-ordered PCE method before propagating the remaining random variables by a Neumann expansion. The limited number of random variables propagated through the PCE would contribute towards the principal variability of the system. The remaining random variables would in turn enrich the response vector. We initially consider the stochastic finite element representation of a systems' stiffness matrix

$$\mathbf{A}(\theta) = \mathbf{A}_0 + \sum_{i=1}^{M} \xi_i(\theta) \mathbf{A}_i \tag{16}$$

In this instance $\mathbf{A}_0 \in \mathbb{R}^{N \times N}$ represents a deterministic, positive definite, symmetric matrix. $\mathbf{A}_i \in \mathbb{R}^{N \times N}$ are general symmetric matrices for $i = 1, 2, \ldots, M$ which contribute towards the stochastic nature of the stiffness matrix and $\xi_i(\theta)$ corresponds to a set of random variables for $i = 1, 2, \ldots, M$. The key is to partition the random variables into two sets

$$\begin{aligned} \mathbf{x}(\theta) &= \{\xi_i(\theta)\}, \qquad i = 1, \ldots, M_1 \\ \mathbf{y}(\theta) &= \{\xi_j(\theta)\}, \qquad j = M_1 + 1, \ldots, M \end{aligned} \tag{17}$$

Hence $\mathbf{x}(\theta)$ and $\mathbf{y}(\theta)$ are vectors of dimensions M_1 and M_2 such that $M_1 + M_2 = M$. Our intention is to construct a polynomial chaos with the vector $\mathbf{x}(\theta)$, and then enriching our solution by performing a Neumann

expansion with the vector $\mathbf{y}(\theta)$. Our formulation exploits the fact that $\mathbf{x}(\theta)$ and $\mathbf{y}(\theta)$ are statistically independent random vectors. By utilising the sets $\mathbf{x}(\theta)$ and $\mathbf{y}(\theta)$, the system matrix can be further decomposed as

$$\mathbf{A}(\theta) = \mathbf{A}_0 + \sum_{i=1}^{M_1} x_i(\theta)\mathbf{A}_i + \sum_{j=1}^{M_2} y_j(\theta)\mathbf{B}_j = \mathbf{A}_y(\theta) + \sum_{i=1}^{M_1} x_i(\theta)\mathbf{A}_i \tag{18}$$

where

$$\mathbf{A}_y(\theta) = \mathbf{A}_0 + \sum_{j=1}^{M_2} y_j(\theta)\mathbf{B}_j \tag{19}$$

is effectively the unvarying contribution seen while considering the PCE with respect to the random variables x_i (which occupy the set $\mathbf{x}(\theta)$). In order to partition the stochastic space in a rational manner, the response of the system when utilising Eq. (3) may be considered. We initially consider the response of (3) in the following form

$$\begin{aligned}\mathbf{u}(\theta) &= \left[\mathbf{A}_0 + \sum_{i=1}^{M} \mathbf{A}_i\xi_i(\theta)\right]^{-1}\mathbf{f}_0 \\ &= \left[\mathbf{I} + \mathbf{A}_0^{-1}\sum_{i=1}^{M} \mathbf{A}_i\xi_i(\theta)\right]^{-1}\underbrace{\mathbf{A}_0^{-1}\mathbf{f}_0}_{\mathbf{u}_0}\end{aligned} \tag{20}$$

where $\mathbf{u}_0$ corresponds to the response of the underlying deterministic system. By applying a first-order expansion method, one has

$$\mathbf{u}(\theta) \approx \left[\mathbf{I} - \mathbf{A}_0^{-1}\sum_{i=1}^{M} \mathbf{A}_i\xi_i(\theta)\right]\mathbf{u}_0 \tag{21}$$

The first-order perturbation is only used to determine the importance of the random components. It is not used to obtain the statistics of the response quantity. Subtracting the response of the underlying deterministic system results in

$$\mathbf{u}(\theta) - \mathbf{u}_0 = -\left[\mathbf{A}_0^{-1}\sum_{i=1}^{M} \mathbf{A}_i\xi_i(\theta)\right]\mathbf{u}_0 \tag{22}$$

By applying a sensitivity analysis with respect to the random variables ξ_i, it is apparent that

$$\frac{\partial}{\partial\xi_i}\left(\mathbf{u}(\theta) - \mathbf{u}_0\right) = -\left[\mathbf{A}_0^{-1}\mathbf{A}_i\right]\mathbf{u}_0 \tag{23}$$

where $\frac{\partial}{\partial\xi_i}$ corresponds to taking the partial derivative with respect to the random variables.

Recall that the vector $\mathbf{u}_0$ is the response vector of the underlying deterministic system. This is not affected by uncertainty in the model. Therefore, the sensitivity of the stochastic response with respect to the ith random variable ξ_i is characterised by the matrix $\mathbf{A}_0^{-1}\mathbf{A}_i$ only. Several matrix norm can be used to explicitly quantify this sensitivity. We use the Frobenius norm and define a scalar parameter

$$\alpha_i = \left\|\mathbf{A}_0^{-1}\mathbf{A}_i\right\|_F \tag{24}$$

where $\|\bullet\|_F$ denotes the Frobenius norm. The scalars α_i are referred to as the *sensitivity norm*. They are subsequently normalised, such that

$$\gamma_i = \frac{\alpha_i}{\sum_{i=1}^{M}\alpha_i} \tag{25}$$

This naturally implies that $\sum_{i=1}^{M}\gamma_i = 1$. The resulting scalars, γ_i, are referred to as the *relative importance factors* of the random components. By considering these relative importance factors, the following inequality can be utilised to partition the stochastic space

$$\gamma_i > h \tag{26}$$

where the value of h is to be appropriately chosen. For the values of i which satisfy the above inequality, the corresponding random variables are to occupy the set $x(\theta)$. If accuracy is of importance, the value of h should be kept low in order for a larger number of the principal random components to be incorporated within the PCE propagation. However if computational speed is of most importance, the value of h should be kept high to incorporate the vast majority of the random variables within the Neumann enrichment.

4.2. An enriched polynomial chaos expansion of the stochastic space

Subsequently to partitioning the stochastic space, it is possible to express the response vector of a stochastic system in the following form

$$\mathbf{u}(\theta) = \sum_{k=1}^{P_1} H_k(\mathbf{x}(\theta))\mathbf{u}_k(\mathbf{y}(\theta)) \tag{27}$$

where $H_k(\boldsymbol{\xi}(\theta))$ are polynomial chaoses and $\mathbf{u}_k(\mathbf{y}(\theta))$ are vectors that need to be determined. The polynomial chaoses are a function of the set $\mathbf{x}(\theta)$, whilst the vectors $\mathbf{u}_k$ are a function of the set $\mathbf{y}(\theta)$. The number of terms arising in the summation is defined by

$$P_1 = \sum_{j=0}^{p}\frac{(M_1 + j - 1)!}{j!(M_1 - 1)!} \tag{28}$$

Eq. (27) captures the essential idea proposed in this study. By allowing the deterministic PCE coefficients to be random, it reduces the 'burden' on the polynomial chaos expansion. The coefficient vectors $\mathbf{u}_k(\mathbf{y}(\theta))$ can be obtained through the following set of $P_1 N \times P_1 N$ equations

$$\left[\widetilde{\mathbf{A}}_0 + \sum_{j=1}^{M_2} y_j(\theta)\widetilde{\mathbf{B}}_j\right]\mathbf{U}_y(\theta) = \mathbf{F} \tag{29}$$

where $\widetilde{\mathbf{A}}_0$, $\widetilde{\mathbf{B}}_j$ and $\mathbf{F}$ are obtained by utilising the underlying PCE approach [2]. The coefficient vectors can then be obtained by noting that

$$\mathbf{U}_y(\theta) = \{\mathbf{u}_{y_1}^T(\theta), \mathbf{u}_{y_2}^T(\theta), \ldots, \mathbf{u}_{y_{P_1}}^T(\theta)\}^T \tag{30}$$

However, solving such a large system for every realisation is computationally very expensive. As a result a Neumann series expansion can be utilised to compute the enriched coefficient vectors. In essence, we aim to compute the following

$$\mathbf{U}_y(\theta) = \left[\widetilde{\mathbf{A}}_0 + \sum_{j=1}^{M_2} y_j(\theta)\widetilde{\mathbf{B}}_j\right]^{-1}\mathbf{F} \tag{31}$$

By employing a Neumann series expansion it is possible to convey $\mathbf{U}_y(\theta)$ as follows

$$\mathbf{U}_y(\theta) = \left[\mathbf{I} - \widetilde{\mathbf{A}}_0^{-1}\sum_{j=1}^{M_2} y_j(\theta)\widetilde{\mathbf{B}}_j + \left(\widetilde{\mathbf{A}}_0^{-1}\sum_{j=1}^{M_2} y_j(\theta)\widetilde{\mathbf{B}}_j\right)^2 - \cdots\right]\mathbf{U}_0 \tag{32}$$

$$= \left[\mathbf{I} + \sum_{k=1}^{\infty}\left(-\widetilde{\mathbf{A}}_0^{-1}\sum_{j=1}^{M_2} y_j(\theta)\widetilde{\mathbf{B}}_j\right)^k\right]\mathbf{U}_0 \tag{33}$$

The series arising in Eq. (33) can be truncated, thus allowing a low-order Neumann series expansion to approximate the vector $\mathbf{U}_y(\theta)$

$$\mathbf{U}_y(\theta) \approx \left[\mathbf{I} + \sum_{k=1}^{P_2}\left(-\widetilde{\mathbf{A}}_0^{-1}\sum_{j=1}^{M_2} y_j(\theta)\widetilde{\mathbf{B}}_j\right)^k\right]\mathbf{U}_0 \tag{34}$$

The number of terms retained in the series, P_2, corresponds to the order of the Neumann series expansion. The number of terms retained can either be pre-defined in order to comply with computational cost, or a convergence criteria can be set

$$\frac{\left\|\left(-\widetilde{\mathbf{A}}_0^{-1}\sum_{j=1}^{M_2} y_j(\theta)\widetilde{\mathbf{B}}_j\right)^{P_2}\right\|}{\left\|\sum_{k=1}^{P_2}\left(-\widetilde{\mathbf{A}}_0^{-1}\sum_{j=1}^{M_2} y_j(\theta)\widetilde{\mathbf{B}}_j\right)^k\right\|} \leq \varepsilon \tag{35}$$

The validity of the inequality must be checked for when additional terms are retained in the series. However, it should be noted that in

order for the Neumann series to converge, the absolute eigenvalues of $\left(-\widetilde{\mathbf{A}}_0^{-1}\sum_{j=1}^{M_2} y_j(\theta)\widetilde{\mathbf{B}}_j\right)^k \quad \forall \quad k = 1,\ldots,P_2$ must be less than one. Through this novel partitioning approach, we expect that including the additional M_2 terms substantially enriches the response vectors, and in turn, better captures the stochastic properties of a randomly parametrised system.

The proposed expression for the PCE coefficients gives an alternative interpretation to their meaning in the context of stochastic response analysis. While employing only a PCE approach, the set of random variables $\mathbf{y}(\theta)$ in Eq. (17) can be considered as 'ignored' or 'missing' variables as the PCE is with $\mathbf{x}(\theta)$ only. From the expression of the response in Eq. (34), therefore, we have

$$\mathbf{U}_y(\theta) \approx \left[\mathbf{I} + \underbrace{\sum_{k=1}^{P_2}\left(-\widetilde{\mathbf{A}}_0^{-1}\sum_{j=1}^{M_2} y_j(\theta)\widetilde{\mathbf{B}}_j\right)^k}_{\text{the contribution of ignored random variables}}\right]\mathbf{U}_0 \tag{36}$$

The consequence of considering the 'additional' set of random variables $\mathbf{y}(\theta)$ is that the coefficients of the classical PCE just need to be 'corrected' as above, leaving the rest of the PCE method unaltered. Therefore, this seemingly minor modification to the classical PCE coefficients allows us to include the effect of possibly large numbers of random variables which would otherwise be ignored or would be computationally too expensive to be included in the original analysis. One can view this as a simple post processing of a classical PCE analysis. This way of viewing Eq. (36) can have a profound impact on the applicability of the PCE analysis in general. For example, one can obtain the PCE coefficients using a non-intrusive or other efficient approaches and then apply the corrections as per Eq. (36) to include the effect of other random variables which were not originally included in the PCE analysis for computational efficiency. Therefore, the proposed scheme presents a balanced approach in comparison to when considering either the PCE or Neumann series expansion approaches individually. For the remainder of this study, the proposed Neumann Enriched Polynomial Chaos Expansion method is given the acronym NEPC.

5. Response statistics

Based upon the methods described in Sections 2 and 4 , this section discusses the first two moments of the response vectors. The moments of the PCE method are initially considered.

5.1. The polynomial chaos expansion: First moment

Due to the deterministic nature of the coefficient vectors, the first moment, which corresponds to the mean of the PCE method can be easily expressed as

$$\mathbb{E}\left\{\mathbf{u}_{PC}(\theta)\right\} = \sum_{k=1}^{P_1}\mathbb{E}\left\{H_k(\mathbf{x}(\theta))\right\}\mathbf{u}_{0_k} = \mathbf{u}_{0_1} \tag{37}$$

where $\mathbb{E}\{*\}$ corresponds to the expected value.

5.2. The polynomial chaos expansion: Second moment

In a similar manner, the deterministic nature of the vectors $\mathbf{u}_{0_k}$ can again be utilised to define the variance of the response vector. The expected value of $\mathbf{u}_{PC}(\theta)\mathbf{u}_{PC}^T(\theta)$ is defined as

$$\mathbb{E}\left\{\mathbf{u}_{PC}(\theta)\mathbf{u}_{PC}^T(\theta)\right\} = \sum_{k=1}^{P_1}\sum_{j=1}^{P_1}\mathbb{E}\left\{H_k(\mathbf{x}(\theta))H_j(\mathbf{x}(\theta))\right\}\mathbf{u}_{0_k}\mathbf{u}_{0_j}^T \tag{38}$$

Due to the orthogonal nature of the polynomial chaoses, it can be deduced that $H_k(\mathbf{x}(\theta))H_j(\mathbf{x}(\theta)) = 0$ when $k \neq j$, thus the above expression can be simplified significantly

$$\mathbb{E}\left\{\mathbf{u}_{PC}(\theta)\mathbf{u}_{PC}^T(\theta)\right\} = \sum_{k=1}^{P_1}\mathbb{E}\left\{H_k^2(\mathbf{x}(\theta))\right\}\mathbf{u}_{0_k}\mathbf{u}_{0_k}^T \tag{39}$$

Thus the variance of the ith element of the response vector can be expressed as

$$\sigma_{u_{PC_i}}^2 = \mathbb{E}\left\{u_{PC}(\theta)u_{PC}^T(\theta)\right\}_i - \mathbb{E}\left\{u_{PC}(\theta)\right\}_i^2 \tag{40}$$

where $\mathbb{E}\left\{u_{PC}(\theta)u_{PC}^T(\theta)\right\}_i$ is the ith diagonal element of the matrix $\mathbb{E}\left\{\mathbf{u}_{PC}(\theta)\mathbf{u}_{PC}^T(\theta)\right\}$ and $\mathbb{E}\left\{u_{PC}(\theta)\right\}_i^2$ is the squared value of the ith element of the vector $\mathbb{E}\left\{\mathbf{u}_{PC}(\theta)\right\}$. If needs be, the standard deviation of the ith element of the response vector can be computed by noting that $\sigma_{u_{PC_i}} = \sqrt{\sigma_{u_{PC_i}}^2}$ where $\sigma_{u_{PC_i}}$ is the standard deviation of the ith element.

5.3. The Neumann enriched polynomial chaos method: First moment

Due to the stochastic nature of both the scalars and the coefficient vectors associated with the NEPC method, the first moment of the response vector of the NEPC method takes the following form

$$\mathbb{E}\left\{\mathbf{u}_{NEPC}(\theta)\right\} = \sum_{k=1}^{P_1}\mathbb{E}\left\{H_k(\mathbf{x}(\theta))\mathbf{u}_{y_k}(\theta)\right\} \tag{41}$$

However, due to the polynomial chaoses and the stochastic vectors being independent from one another, the expected value operator can been treated as a multiplicative function, hence

$$\mathbb{E}\left\{\mathbf{u}_{NEPC}(\theta)\right\} = \sum_{k=1}^{P_1}\mathbb{E}\left\{H_k(\mathbf{x}(\theta))\right\}\mathbb{E}\left\{\mathbf{u}_{y_k}(\theta)\right\} \tag{42}$$

where the expected values of the stochastic $\mathbf{u}_{y_k}(\theta)$ vectors can be computed from

$$\begin{aligned}\mathbb{E}\left\{\mathbf{U}_y(\theta)\right\} &= \mathbb{E}\left[\mathbf{u}_{y_1}^T(\theta)\ \mathbf{u}_{y_2}^T(\theta)\ldots\mathbf{u}_{y_{P_1}}^T(\theta)\right]^T \\ &= \left[\mathbb{E}\left\{\mathbf{u}_{y_1}^T(\theta)\right\}\ \mathbb{E}\left\{\mathbf{u}_{y_2}^T(\theta)\right\}\ldots\mathbb{E}\left\{\mathbf{u}_{y_{P_1}}^T(\theta)\right\}\right]^T\end{aligned} \tag{43}$$

For notational convenience, the matrix $\mathbf{U}_y(\theta)$ can be redefined

$$\mathbf{U}_y(\theta) = \left[\mathbf{I} + \sum_{k=1}^{P_2}(-1)^k\Gamma_k(\theta)\right]\mathbf{U}_0 \tag{44}$$

where $\Gamma_k(\theta) = \left(\widetilde{\mathbf{A}}_0^{-1}\sum_{j=1}^{M_2} y_j(\theta)\widetilde{\mathbf{B}}_j\right)^k$. Thus by taking the expected value of the matrix $\mathbf{U}_y(\theta)$, it is apparent that the variable $\Gamma_k(\theta)$ contains all the stochastic properties of the matrix

$$\begin{aligned}\mathbb{E}\left\{\mathbf{U}_y(\theta)\right\} &= \mathbb{E}\left\{\left[\mathbf{I} + \sum_{k=1}^{P_2}(-1)^k\Gamma_k(\theta)\right]\mathbf{U}_0\right\} \\ &= \left[\mathbf{I} + \sum_{k=1}^{P_2}(-1)^k\mathbb{E}\left\{\Gamma_k(\theta)\right\}\right]\mathbf{U}_0\end{aligned} \tag{45}$$

The number of terms retained in the summation, P_2, corresponds to the order of the Neumann expansion. We initially consider the cases for when $P_2 = 1$ and $P_2 = 2$. In order to gain an expression for the mean of the response vector when a first order Neumann expansion is utilised, the expected value of $\Gamma_1(\theta)$ needs to be explored

$$\begin{aligned}\mathbb{E}\left\{\Gamma_1(\theta)\right\} &= \mathbb{E}\left\{\widetilde{\mathbf{A}}_0^{-1}\sum_{j_1=1}^{M_2} y_{j_1}(\theta)\widetilde{\mathbf{B}}_{j_1}\right\} \\ &= \widetilde{\mathbf{A}}_0^{-1}\sum_{j_1=1}^{M_2}\mathbb{E}\left\{y_{j_1}(\theta)\right\}\widetilde{\mathbf{B}}_{j_1}\end{aligned} \tag{46}$$

Due to $y_j(\theta)$ being a Gaussian random variable, it can be deduced that $\mathbb{E}\left\{y_{j_1}(\theta)\right\} = 0$. Thus by combining the result of Eq. (46) with Eq. (45), it is apparent that performing a NEPC with a first order Neumann expansion does not enrich the approximation of the mean of the response vector in comparison to the PCE method. In a similar manner, the expected value of the mean of the approximated response vector is explored when $P_2 = 2$. It has already been ascertained that $\mathbb{E}\left\{\Gamma_1(\theta)\right\} = 0$, therefore the expected value of $\Gamma_2(\theta)$ is considered

$$\mathbb{E}\left\{\Gamma_2(\theta)\right\} = \mathbb{E}\left\{\left(\widetilde{\mathbf{A}}_0^{-1}\sum_{j=1}^{M_2} y_j(\theta)\widetilde{\mathbf{B}}_j\right)^2\right\} = \widetilde{\mathbf{A}}_0^{-1}\sum_{j_1=1}^{M_2}\sum_{j_2=1}^{M_2}\mathbb{E}\left\{y_{j_1}(\theta)y_{j_2}(\theta)\right\}\widetilde{\mathbf{B}}_{j_1}\widetilde{\mathbf{A}}_0^{-1}\widetilde{\mathbf{B}}_{j_2} \tag{47}$$

It can be noted that $\mathbb{E}\left\{y_{j_1}(\theta)y_{j_2}(\theta)\right\} = 0$ when $j_1 \neq j_2$, thus the expression for $\mathbb{E}\left\{\Gamma_2(\theta)\right\}$ can be simplified to

$$\mathbb{E}\left\{\Gamma_2(\theta)\right\} = \widetilde{\mathbf{A}}_0^{-1}\sum_{j=1}^{M_2}\mathbb{E}\left\{y_j^2(\theta)\right\}\widetilde{\mathbf{B}}_j\widetilde{\mathbf{A}}_0^{-1}\widetilde{\mathbf{B}}_j \tag{48}$$

Therefore, it is apparent that the second term arising in the summation contained within Eq. (45) enriches the mean of the response vector. In turn, the induced error is reduced. To gain a general overview of the nature of the terms arising in the summation when $P_2 > 2$, the general case for Γ_r is considered

$$\mathbb{E}\left\{\Gamma_r(\theta)\right\} = \mathbb{E}\left\{\left(\widetilde{\mathbf{A}}_0^{-1}\sum_{j=1}^{M_2} y_j(\theta)\widetilde{\mathbf{B}}_j\right)^r\right\} = \widetilde{\mathbf{A}}_0^{-1}\sum_{j_1=1}^{M_2}\sum_{j_2=1}^{M_2}\cdots\sum_{j_r=1}^{M_2}\mathbb{E}\left\{y_{j_1}(\theta)y_{j_2}(\theta)\ldots y_{j_r}(\theta)\right\}\widetilde{\mathbf{B}}_{j_1}\widetilde{\mathbf{A}}_0^{-1}\widetilde{\mathbf{B}}_{j_2}\ldots\widetilde{\mathbf{A}}_0^{-1}\widetilde{\mathbf{B}}_{j_r} \tag{49}$$

By combining the above expression with the following relationship [44]

$$\mathbb{E}\left\{y_j^r\right\} = \begin{cases} 0, & \text{if } r \text{ is odd.} \\ \sigma^r(r-1)!!, & \text{if } r \text{ is even.} \end{cases} \tag{50}$$

it is apparent that $\mathbb{E}\left\{\Gamma_r(\theta)\right\} = 0$ when the value of r is odd. Therefore, in order to enrich the mean of the response vector, considering a Neumann Expansion with a odd valued order (r) is needless. Considering an order of $r-1$ would be sufficient and computationally less expensive. However, by incorporating the properties of the Hermite polynomials, it can be deduced that the first moment of the NEPC method can be expressed as

$$\mathbb{E}\left\{\mathbf{u}_{NEPC}(\theta)\right\} = \mathbb{E}\left\{\mathbf{u}_{y_1}(\theta)\right\} \tag{51}$$

where $\mathbb{E}\left\{\mathbf{u}_{y_1}(\theta)\right\}$ is contained within $\mathbb{E}\left\{\mathbf{U}_y(\theta)\right\}$ as shown by Eq. (43).

5.4. The Neumann enriched polynomial chaos method: Second moment

To analyse the nature of the variance of the response vector, the expected value of $\mathbf{u}_{NEPC}(\theta)\mathbf{u}_{NEPC}^T(\theta)$ must be examined

$$\mathbb{E}\left\{\mathbf{u}_{NEPC}(\theta)\mathbf{u}_{NEPC}^T(\theta)\right\} = \sum_{k=1}^{P_1}\sum_{j=1}^{P_1}\mathbb{E}\left\{H_k(\mathbf{x}(\theta))H_j(\mathbf{x}(\theta))\mathbf{u}_{y_k}(\theta)\mathbf{u}_{y_j}^T(\theta)\right\} \tag{52}$$

By utilising the orthogonal nature of the polynomial chaoses and the multiplicative nature of the expected value operator, Eq. (52) can be expressed as

$$\mathbb{E}\left\{\mathbf{u}_{NEPC}(\theta)\mathbf{u}_{NEPC}^T(\theta)\right\} = \sum_{k=1}^{P_1}\mathbb{E}\left\{H_k^2(\mathbf{x}(\theta))\right\}\mathbb{E}\left\{\mathbf{u}_{y_k}(\theta)\mathbf{u}_{y_k}^T(\theta)\right\} \tag{53}$$

The result of $\mathbb{E}\left\{H_k^2(\mathbf{x}(\theta))\right\}$ produces a scalar value for all values of k, whilst $\mathbb{E}\left\{\mathbf{u}_{y_k}(\theta)\mathbf{u}_{y_k}^T(\theta)\right\}$ produces an $N \times N$ matrix $\forall\, k$, where N corresponds to the number of degrees of freedom associated with the given structure. In order to assess the nature of $\mathbb{E}\left\{\mathbf{u}_{y_k}(\theta)\mathbf{u}_{y_k}^T(\theta)\right\}$, we initially consider the expected value of $\mathbf{U}_y(\theta)\mathbf{U}_y^T(\theta)$

$$\mathbb{E}\left\{\mathbf{U}_y(\theta)\mathbf{U}_y^T(\theta)\right\} = \left[\mathbf{I} + \sum_{k_1=1}^{P_2}(-1)^{k_1}\Gamma_{k_1}(\theta)\right]\mathbf{U}_0\mathbf{U}_0^T\left[\mathbf{I} + \sum_{k_2=1}^{P_2}(-1)^{k_2}\Gamma_{k_2}(\theta)\right]^T \tag{54}$$

where $\Gamma_k(\theta) = \left(\widetilde{\mathbf{A}}_0^{-1}\sum_{j=1}^{M_2} y_j(\theta)\widetilde{\mathbf{B}}_j\right)^k$ is defined for notational convenience. By defining $\mathbf{P}_0 = \mathbf{U}_0\mathbf{U}_0^T$, Eq. (54) can be expressed as

$$\begin{aligned}\mathbb{E}\left\{\mathbf{U}_y(\theta)\mathbf{U}_y^T(\theta)\right\} &= \mathbb{E}\left\{\left[\mathbf{P}_0 + \left(\sum_{k_1=1}^{P_2}(-1)^{k_1}\Gamma_{k_1}(\theta)\right)\mathbf{P}_0\right]\left[\mathbf{I} + \sum_{k_2=1}^{P_2}(-1)^{k_2}\Gamma_{k_2}(\theta)\right]^T\right\} \\ &= \mathbf{P}_0 + \left[\sum_{k=1}^{P_2}(-1)^k\mathbb{E}\left\{\Gamma_k(\theta)\right\}\right]\mathbf{P}_0 + \mathbf{P}_0\sum_{k=1}^{P_2}(-1)^k\mathbb{E}\left\{\Gamma_k^T(\theta)\right\} \\ &\quad + \sum_{k_1=1}^{P_2}\sum_{k_2=1}^{P_2}(-1)^{k_1+k_2}\mathbb{E}\left\{\Gamma_{k_1}(\theta)\mathbf{P}_0\Gamma_{k_2}^T(\theta)\right\}\end{aligned} \tag{55}$$

Similarly to the discussion held for the mean of the response vector, we initially consider the cases when $P_2 = 1$ and $P_2 = 2$. When $P_2 = 1$, it is apparent that $\mathbb{E}\left\{\Gamma_1\right\} = 0$ from Eq. (46). By also noting that $\mathbb{E}\left\{y_{j_1}(\theta)y_{j_2}(\theta)\right\} = 0$ when $j_1 \neq j_2$, it is apparent that

$$\begin{aligned}\mathbb{E}\left\{\Gamma_1(\theta)\mathbf{P}_0\Gamma_1^T(\theta)\right\} &= \mathbb{E}\left\{\left(\widetilde{\mathbf{A}}_0^{-1}\sum_{j_1=1}^{M_2} y_{j_1}(\theta)\widetilde{\mathbf{B}}_{j_1}\right)\mathbf{P}_0\left(\widetilde{\mathbf{A}}_0^{-1}\sum_{k_1=1}^{M_2} y_{k_1}(\theta)\widetilde{\mathbf{B}}_{k_1}\right)^T\right\} \\ &= \widetilde{\mathbf{A}}_0^{-1}\left[\sum_{j=1}^{M_2}\mathbb{E}\left\{y_j^2(\theta)\right\}\widetilde{\mathbf{B}}_j\mathbf{P}_0\widetilde{\mathbf{B}}_j^T\right]\widetilde{\mathbf{A}}_0^{-T}\end{aligned} \tag{56}$$

Thus resulting in

$$\mathbb{E}\left\{\mathbf{U}_y(\theta)\mathbf{U}_y^T(\theta)\right\} = \mathbf{P}_0 + \widetilde{\mathbf{A}}_0^{-1}\left[\sum_{j=1}^{M_2}\mathbb{E}\left\{y_j^2(\theta)\right\}\widetilde{\mathbf{B}}_j\mathbf{P}_0\widetilde{\mathbf{B}}_j^T\right]\widetilde{\mathbf{A}}_0^{-T} \tag{57}$$

The $\mathbb{E}\left\{\mathbf{u}_{y_k}(\theta)\mathbf{u}_{y_k}^T(\theta)\right\}$ matrices $\forall\, k$ can be obtained from the result of Eq. (57). The matrices $\mathbb{E}\left\{\mathbf{u}_{y_k}(\theta)\mathbf{u}_{y_k}^T(\theta)\right\}$ form diagonal block matrices contained within the matrix $\mathbb{E}\left\{\mathbf{U}_y(\theta)\mathbf{U}_y^T(\theta)\right\}$. When a second order Neumann expansion approach is utilised, the expectation of the matrix $\mathbf{U}_y(\theta)\mathbf{U}_y^T(\theta)$ takes the following form

$$\mathbb{E}\left\{\mathbf{U}_y(\theta)\mathbf{U}_y^T(\theta)\right\} = \mathbf{P}_0 + \mathbb{E}\left\{\Gamma_2(\theta)\right\}\mathbf{P}_0 + \mathbf{P}_0\mathbb{E}\left\{\Gamma_2^T(\theta)\right\} + \sum_{k=1}^{2}\mathbb{E}\left\{\Gamma_k(\theta)\mathbf{P}_0\Gamma_k^T(\theta)\right\} \tag{58}$$

where

$$\mathbb{E}\left\{\Gamma_2(\theta)\right\} = \widetilde{\mathbf{A}}_0^{-1}\sum_{j=1}^{M_2}\mathbb{E}\left\{y_j^2(\theta)\right\}\widetilde{\mathbf{B}}_j\widetilde{\mathbf{A}}_0^{-1}\widetilde{\mathbf{B}}_j \tag{59}$$

$$\mathbb{E}\left\{\Gamma_2^T(\theta)\right\} = \left[\sum_{j=1}^{M_2}\mathbb{E}\left\{y_j^2(\theta)\right\}\widetilde{\mathbf{B}}_j^T\widetilde{\mathbf{A}}_0^{-T}\widetilde{\mathbf{B}}_j^T\right]\widetilde{\mathbf{A}}_0^{-T} \tag{60}$$

and

$$\begin{aligned}\mathbb{E}\left\{\Gamma_2(\theta)\mathbf{P}_0\Gamma_2^T(\theta)\right\} &= \mathbb{E}\left\{\left(\widetilde{\mathbf{A}}_0^{-1}\sum_{j_1=1}^{M_2}\sum_{j_2=1}^{M_2} y_{j_1}(\theta)y_{j_2}(\theta)\widetilde{\mathbf{B}}_{j_1}\widetilde{\mathbf{A}}_0^{-1}\widetilde{\mathbf{B}}_{j_2}\right)\mathbf{P}_0\right. \\ &\qquad \left.\left(\widetilde{\mathbf{A}}_0^{-1}\sum_{k_1=1}^{M_2}\sum_{k_2=1}^{M_2} y_{k_1}(\theta)y_{k_2}(\theta)\widetilde{\mathbf{B}}_{k_1}\widetilde{\mathbf{A}}_0^{-1}\widetilde{\mathbf{B}}_{k_2}\right)^T\right\} \\ &= \widetilde{\mathbf{A}}_0^{-1}\left[\sum_{j=1}^{M_2}\mathbb{E}\left\{y_j^4(\theta)\right\}\widetilde{\mathbf{B}}_j\widetilde{\mathbf{A}}_0^{-1}\widetilde{\mathbf{B}}_j\mathbf{P}_0\widetilde{\mathbf{B}}_j^T\widetilde{\mathbf{A}}_0^{-T}\widetilde{\mathbf{B}}_j^T + \right. \\ &\qquad \sum_{j=1}^{M_2}\sum_{k=1}^{M_2}\mathbb{E}\left\{y_j^2(\theta)y_k^2(\theta)\right\}\left[\widetilde{\mathbf{B}}_j\widetilde{\mathbf{A}}_0^{-1}\widetilde{\mathbf{B}}_j\mathbf{P}_0\widetilde{\mathbf{B}}_k^T\widetilde{\mathbf{A}}_0^{-T}\widetilde{\mathbf{B}}_k^T + \right. \\ &\qquad \left.\left.\widetilde{\mathbf{B}}_j\widetilde{\mathbf{A}}_0^{-1}\widetilde{\mathbf{B}}_k\mathbf{P}_0\widetilde{\mathbf{B}}_j^T\widetilde{\mathbf{A}}_0^{-T}\widetilde{\mathbf{B}}_k^T + \widetilde{\mathbf{B}}_j\widetilde{\mathbf{A}}_0^{-1}\widetilde{\mathbf{B}}_k\mathbf{P}_0\widetilde{\mathbf{B}}_k^T\widetilde{\mathbf{A}}_0^{-T}\widetilde{\mathbf{B}}_j^T\right]\right]\widetilde{\mathbf{A}}_0^{-T}\end{aligned} \tag{61}$$

The expression for $\mathbb{E}\left\{\Gamma_1(\theta)\mathbf{P}_0\Gamma_1^T(\theta)\right\}$ is given by Eq. (56). It can be intuitively deduced that $\mathbb{E}\left\{\Gamma_1(\theta)\right\} = \mathbb{E}\left\{\Gamma_1^T(\theta)\right\} = \mathbb{E}\left\{\Gamma_1(\theta)\mathbf{P}_0\Gamma_2^T(\theta)\right\} =$

$\mathbb{E}\left\{\Gamma_2(\theta)\mathbf{P}_0\Gamma_1^T(\theta)\right\} = 0$. Similarly to the previous case, the $\mathbb{E}\left\{\mathbf{u}_{y_k}(\theta)\mathbf{u}_{y_k}^T(\theta)\right\}$ matrices $\forall\ k$ can be obtained from the diagonal block matrices contained within the matrix $\mathbb{E}\left\{\mathbf{U}_y(\theta)\mathbf{U}_y^T(\theta)\right\}$. Contrary to the mean of the response vector, it is apparent that considering a Neumann Expansion with an odd valued order enriches the variance of the response vector. This can be adjudged by re-examining the generic case stated in Eq. (55). When considering the last term arising in $\sum_{k_1=1}^{P_2}\sum_{k_2=1}^{P_2}(-1)^{k_1+k_2}\mathbb{E}\left\{\Gamma_{k_1}(\theta)\mathbf{P}_0\Gamma_{k_2}^T(\theta)\right\}$, it can be deduced that

$$\mathbb{E}\left\{\Gamma_{P_2}(\theta)\Gamma_{P_2}^T(\theta)\right\} = \widetilde{\mathbf{A}}_0^{-1}\left[\sum_{j_1=1}^{M_2}\sum_{j_2=1}^{M_2}\cdots\sum_{j_{P_2}=1}^{M_2}\sum_{k_1=1}^{M_2}\sum_{k_2=1}^{M_2}\cdots\sum_{k_{P_2}=1}^{M_2}\mathbb{E}\left\{y_{j_1}(\theta)y_{j_2}(\theta)\cdots y_{j_{P_2}}(\theta)y_{k_1}(\theta)y_{k_2}(\theta)\cdots y_{k_{P_2}}(\theta)\right\}\widetilde{\mathbf{B}}_{j_1}\widetilde{\mathbf{A}}_0^{-1}\widetilde{\mathbf{B}}_{j_2}\cdots\widetilde{\mathbf{A}}_0^{-1}\widetilde{\mathbf{B}}_{j_{P_2}}\widetilde{\mathbf{B}}_{k_{P_2}}^T\widetilde{\mathbf{A}}_0^{-T}\cdots\widetilde{\mathbf{B}}_{k_2}^T\widetilde{\mathbf{A}}_0^{-T}\widetilde{\mathbf{B}}_{k_1}^T\right]\widetilde{\mathbf{A}}_0^{-T} \tag{62}$$

When $y_{j_1}(\theta) = y_{j_2}(\theta) = \ldots = y_{j_{P_2}}(\theta) = y_{k_1}(\theta) = y_{k_2}(\theta) = y_{k_{P_2}}(\theta)$ it is evident that

$$\mathbb{E}\left\{y_{j_1}(\theta)y_{j_2}(\theta)\ldots y_{j_{P_2}}(\theta)y_{k_1}(\theta)y_{k_2}(\theta)\ldots y_{k_{P_2}}(\theta)\right\} = \mathbb{E}\left\{y^{2P_2}(\theta)\right\} = \sigma^{2P_2}(2P_2-1)!! \tag{63}$$

Therefore it is apparent that $\sum_{k_1=1}^{P_2}\sum_{k_2=1}^{P_2}(-1)^{k_1+k_2}\mathbb{E}\left\{\Gamma_{k_1}(\theta)\mathbf{P}_0\Gamma_{k_2}^T(\theta)\right\} \neq 0$ irrespective of P_2 being an odd or an even number. In turn, it can be deduced that the value of $\mathbb{E}\left\{\mathbf{u}_{NEPC}(\theta)\mathbf{u}_{NEPC}^T(\theta)\right\}$ will be enriched for every value of P_2 as P_2 is increased. As with the case of the PCE method, the variance of the ith element of the response vector is defined as

$$\sigma_{u_{NEPC_i}}^2 = \mathbb{E}\left\{u_{NEPC}(\theta)u_{NEPC}^T(\theta)\right\}_i - \mathbb{E}\left\{u_{NEPC}(\theta)\right\}_i^2 \tag{64}$$

where $\mathbb{E}\left\{u_{NEPC}(\theta)u_{NEPC}^T(\theta)\right\}_i$ is the ith diagonal element of the matrix $\mathbb{E}\left\{\mathbf{u}_{NEPC}(\theta)\mathbf{u}_{NEPC}^T(\theta)\right\}$ and $\mathbb{E}\left\{u_{NEPC}(\theta)\right\}_i^2$ is the squared value of the ith element of the vector $\mathbb{E}\left\{\mathbf{u}_{NEPC}(\theta)\right\}$. The standard deviation of the ith element of the response vector can be computed by

$$\sigma_{u_{NEPC_i}} = \sqrt{\sigma_{u_{NEPC_i}}^2} \tag{65}$$

where $\sigma_{u_{NEPC_i}}$ is the standard deviation of the ith element.

6. Numerical examples

Thus far a potentially promising method which enriches the coefficient vectors that are associated with the PCE method has been suggested. In this section the proposed method is applied to analyse the bending of twelve Euler–Bernoulli cantilever beams which have stochastic properties and a flow through a stochastic porous media. The results obtained when utilising the proposed scheme are compared with the responses obtained when using the classical PCE method and the benchmark DMCS method. Thus the following three methods are employed.

- Direct Monte Carlo Simulation [DMCS] with full set of random variables:
  $\mathbf{u}(\theta) = \mathbf{A}^{-1}(\theta)\mathbf{f}_0$
- Classical Polynomial Chaos Expansion [PC] with random variables in partition $\mathbf{x}$ only:
  $\mathbf{u}(\theta) \approx \sum_{k=1}^{P_1} H_k(\mathbf{x}(\theta))\mathbf{u}_{0_k}$
- Neumann Enriched Polynomial Chaos Expansion [NEPC] with full set of random variables:
  $\mathbf{u}(\theta) \approx \sum_{k=1}^{P_1} H_k(\mathbf{x}(\theta))\mathbf{u}_{y_k}(\theta)$

6.1. Euler–Bernoulli cantilever beams

All the beams under consideration are 1.00 m in length (L), and have a rectangular cross-section of width 0.03 m and height 0.003 m.

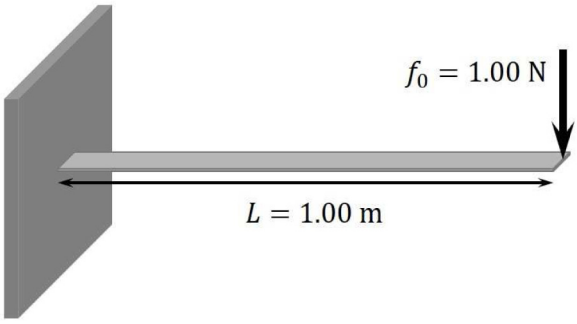

Fig. 1. The configuration of the stochastically parametrised cantilever beams.

Fig. 1 illustrates the configuration. Through the use of the stochastic finite element method, the beams have been discretised into 100 elements. Due to the beams being clamped, the displacement and rotational degrees of freedom at the clamped ends are zero. A deterministic vertical static point load of magnitude $f_0 = 1.00$ N is exerted at the free tip of each beam.

The deterministic values of the Young's modulus and the second moment of area for each beam are $E_0 = 2\times10^{11}$ Nm^{-2} and $I_0 = 1.25\times10^{-10}$ m^4 respectively. The chosen value for the Young's modulus corresponds to steel. The bending rigidity of the beams, EI, is assumed to be a stationary Gaussian random field of the following form

$$EI(x,\theta) = EI_0(1 + a(x,\theta)) \tag{66}$$

where EI_0 denotes the mean value of the bending rigidity. The function $a(\mathbf{x},\theta)$ represents the stationary Gaussian random field which has a mean of zero. The notation $\mathbf{x}$ corresponds to the coordinate direction along the length of the beam. The autocovariance kernel of the random field is given by

$$C(x_1,x_2) = e^{-(|x_1-x_2|)/\mu} \tag{67}$$

where μ is the correlation length. Three different values for the correlation length are considered: $\mu = \{L, L/25, L/50\}$. Varying the value of μ results in models which require a different number of terms retained in the Karhunen–Loève expansion. Having a small correlation length requires the retention of more terms. Consequently, the size of the linear system associated with the PC and NEPC methods will be extremely large due to the result of Eq. (7). In turn, each value of correlation length has been modelled for four different input values of the standard deviation: $\sigma_a = \{0.05, 0.10, 0.15, 0.20\}$. This allows for the methods to be compared under different levels of uncertainty. This results in twelve different configurations.

The number of terms retained in each of the configurations' Karhunen–Loève expansions have been computed by analysing the decaying nature of the eigenvalues that arise in Eq. (2). The terms which satisfy the following inequality have been retained

$$\frac{\nu_j}{\nu_1} \geq \varepsilon_2 \tag{68}$$

where ν_1 is the value of the largest eigenvalue and ν_j the value of the jth eigenvalue. The tolerance value ε_2 is to be selected appropriately. For the given numerical example, ε_2 has been set to 0.10. Thus for the twelve configuration, the following number of terms have been retained in the Karhunen–Loève expansions (see Table 3).

For the virtue of comparing, the value of M_1 (the number of random variables associated with the polynomial chaos contribution) has been fixed to 2 for all configurations. As a result, the value of M_2 (the number of additional random terms associated with the enriching method) equates to $M-2$, where the value of M corresponds to the number of terms retained in the respective Karhunen–Loève expansions. 10,000 Monte Carlo simulation samples are considered for each configuration.

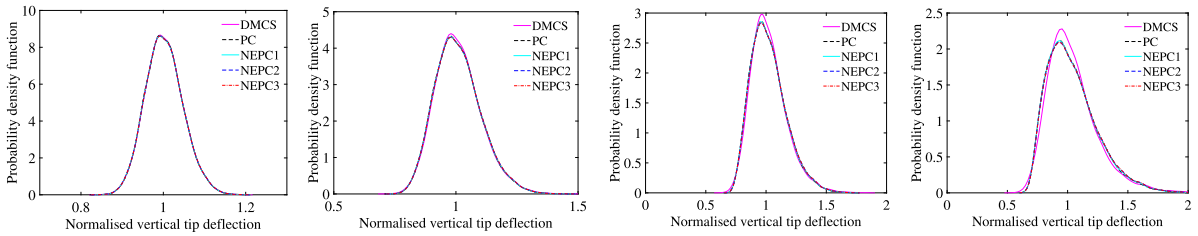

(a) $\sigma_a = 0.05$ (b) $\sigma_a = 0.10$ (c) $\sigma_a = 0.15$ (d) $\sigma_a = 0.20$

Fig. 2. The probability density function of the vertical displacement at the tip of the beam. The response is shown for all values of the standard deviation of the bending rigidity $\sigma_a = \{0.05, 0.10, 0.15, 0.20\}$ when the correlation length is set at $\mu = L$.

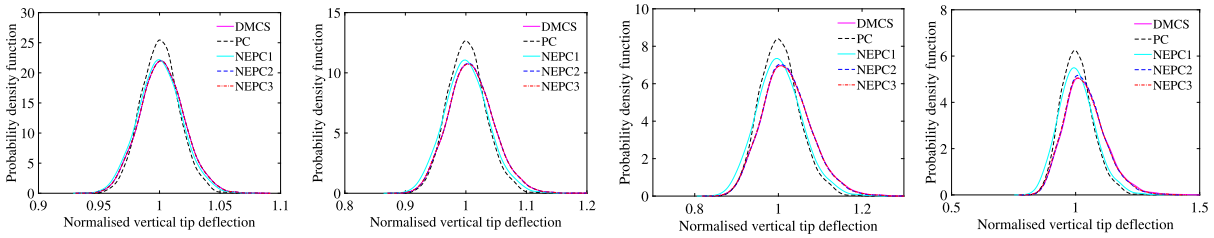

(a) $\sigma_a = 0.05$ (b) $\sigma_a = 0.10$ (c) $\sigma_a = 0.15$ (d) $\sigma_a = 0.20$

Fig. 3. The probability density function of the vertical displacement at the tip of the beam. The response is shown for all values of the standard deviation of the bending rigidity $\sigma_a = \{0.05, 0.10, 0.15, 0.20\}$ when the correlation length is set at $\mu = L/25$.

Table 3
The number of terms retained in the Karhunen–Loève expansions whilst employing the NEPC methods.

		Standard deviation			
		0.05	0.10	0.15	0.20
Correlation length	L	4	4	4	4
	$L/25$	36	36	36	36
	$L/50$	71	71	71	71

It has been verified that using 10,000 samples gives a satisfactory convergence for the first two moments of the quantities of interest.

Figs. 2, 3 and 4 illustrate the normalised probability density function of the deflection at the tip of the beam for all twelve configurations. The normalisation factor corresponds to $\frac{f_0 L^3}{3EI_0}$ where f_0 is the magnitude of the static point force which is placed at the tip of the beam. All the methods have initially been implemented with second order polynomial chaoses. The PC method has incorporated M_1 terms from the Karhunen–Loève expansions, thus the enriched NEPC methods incorporate an additional M_2 terms. If the PC method were to incorporate the same number of random variables as the NEPC methods, the size of the linear system which would require solving could become infeasibly large. When considering the cases which have a correlation length of $L/50$, a $525,600 \times 525,600$ system would be required to be solved if M terms were to be retained in the PC method. In our cases, both the PC and NEPC methods require a $1,200 \times 1,200$ sized system to be solved only once. For the NEPC methods, three different values for the order of the Neumann series expansion have been considered. NEPC1 has incorporated a first order expansion, whilst NEPC2 and NEPC3 have incorporated a second and third order expansion respectively. These have been presented in order to illustrate the effect of varying the order of the Neumann series expansion.

When analysing Fig. 2 it is apparent that all the reduced methods produce probability density functions which mimics the benchmark approach when $\sigma_a = 0.05$. However when $\sigma_a = 0.20$, a clear discrepancy is visible between the reduced methods and the benchmark solution. Since the enriching methods do not visibly improve upon the PC method, it can be concluded that the majority of the induced error seen in the normalised probability density function of the deflection at the tip of the beam can be contributed to the order of the polynomial chaoses. When the correlation length is reduced, a clear improvement can be seen when the NEPC methods are implemented in comparison to the PC method. This is most apparent when $\mu_a = L/50$. The NEPC1 method visually appears to improve the second moment, whilst the NEPC2 method visually appears to improve both the first and second moments of the normalised deflection at the tip of the beam. This coincides with the discussion held in Section 5.

To analyse the error arising from the mean of the normalised response vector, the normalised approximate L^2 relative error is considered. This enables the error arising from the mean of the normalised response vector to be characterised by a single value. The approximate L^2 relative error of the mean of the normalised response vector is defined as

$$\hat{\varepsilon}^{\boldsymbol{\mu}}_{L^2} = \frac{\|\boldsymbol{\mu}_{DMCS} - \boldsymbol{\mu}_{CM}\|_{L^2}}{\|\boldsymbol{\mu}_{DMCS}\|_{L^2}} \tag{69}$$

where $\boldsymbol{\mu}_{DMCS}$ denotes the mean of the response vector obtained by using the benchmark DMCS method and $\boldsymbol{\mu}_{CM}$ the mean of the response vector obtained by a comparable method. The normalised approximate L^2 relative error has been explored for different orders of the Neumann expansion and for different orders of the polynomial chaoses. All twelve cantilever beams cases have been depicted in Figs. 5, 6 and 7. Six different values for the orders of the Neumann series expansion are given along the x-axis. The case of when the order equates to zero corresponds to the classical PC method. Three different values for the order of the polynomial chaoses are explored. "OPC = 1" corresponds to the first order, "OPC = 2" to the second and "OPC = 3" corresponds to the third.

It is apparent that the effect of increasing the order of the polynomial chaos diminishes as both the correlation length decreases and as the value of the standard deviation increases. Thus if the correlation length is sufficiently small a low-ordered polynomial chaos expansion is sufficient in conjunction with the proposed enrichment method. The step wise nature of the normalised approximate L^2 relative error consolidates that using an odd valued order for the Neumann series expansion is purposeless. Using an order that corresponds to the previous

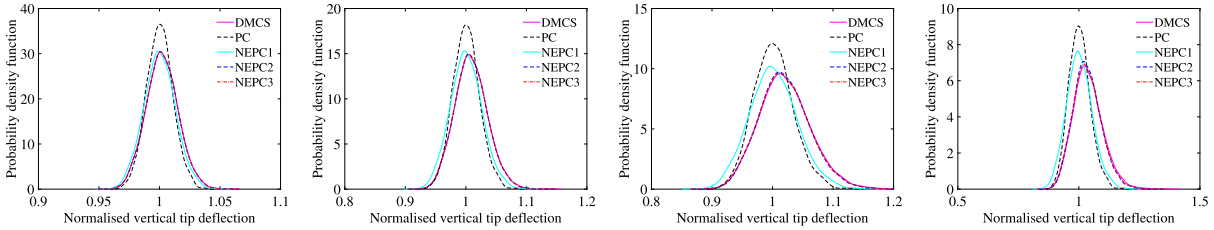

(a) $\sigma_a = 0.05$ (b) $\sigma_a = 0.10$ (c) $\sigma_a = 0.15$ (d) $\sigma_a = 0.20$

Fig. 4. The probability density function of the vertical displacement at the tip of the beam. The response is shown for all values of the standard deviation of the bending rigidity $\sigma_a = \{0.05, 0.10, 0.15, 0.20\}$ when the correlation length is set at $\mu = L/50$.

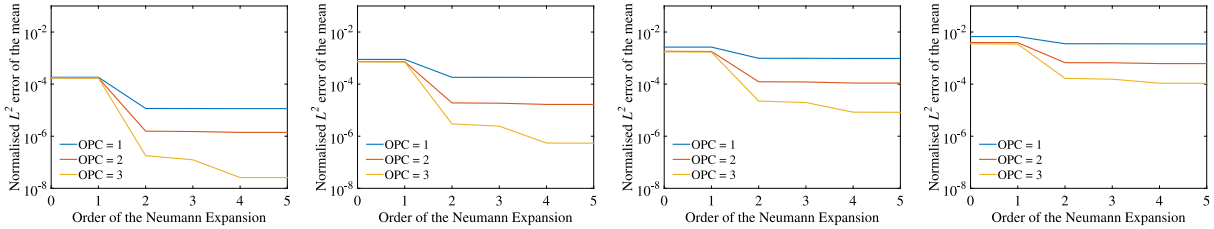

(a) $\sigma = 0.05$ (b) $\sigma = 0.10$ (c) $\sigma = 0.15$ (d) $\sigma = 0.20$

Fig. 5. The normalised approximate L^2 relative error of the mean of the response vector for all values of the standard deviation of the bending rigidity $\sigma_a = \{0.05, 0.10, 0.15, 0.20\}$. The normalised approximate L^2 relative error of the mean of the response vector has been depicted for different orders of the polynomial chaos expansion ($P_1 = \{1, 2, 3\}$) and for different orders of the Neumann expansion ($P_2 = \{0, 1, 2, 3, 4, 5\}$) when the correlation length is set at $\mu = L$.

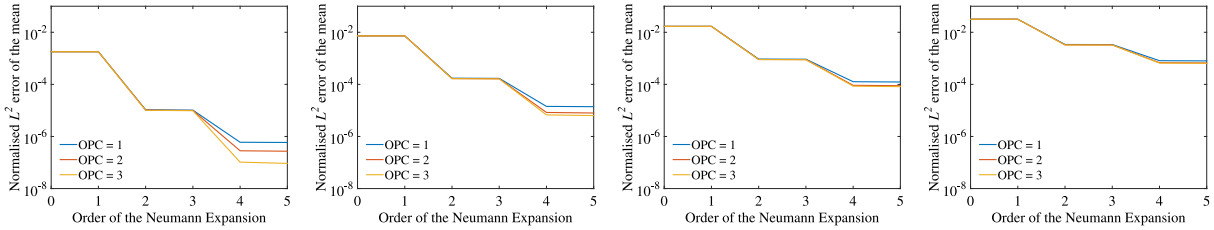

(a) $\sigma = 0.05$ (b) $\sigma = 0.10$ (c) $\sigma = 0.15$ (d) $\sigma = 0.20$

Fig. 6. The normalised approximate L^2 relative error of the mean of the response vector for all values of the standard deviation of the bending rigidity $\sigma_a = \{0.05, 0.10, 0.15, 0.20\}$. The normalised approximate L^2 relative error of the mean of the response vector has been depicted for different orders of the polynomial chaos expansion ($P_1 = \{1, 2, 3\}$) and for different orders of the Neumann expansion ($P_2 = \{0, 1, 2, 3, 4, 5\}$) when the correlation length is set at $\mu = L/25$.

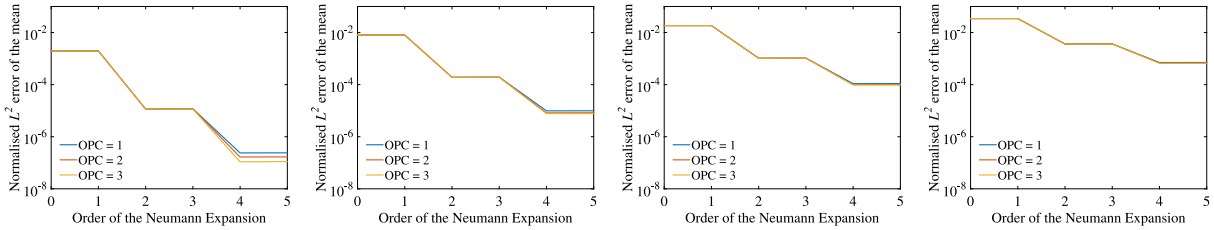

(a) $\sigma = 0.05$ (b) $\sigma = 0.10$ (c) $\sigma = 0.15$ (d) $\sigma = 0.20$

Fig. 7. The normalised approximate L^2 relative error of the mean of the response vector for all values of the standard deviation of the bending rigidity $\sigma_a = \{0.05, 0.10, 0.15, 0.20\}$. The normalised approximate L^2 relative error of the mean of the response vector has been depicted for different orders of the polynomial chaos expansion ($P_1 = \{1, 2, 3\}$) and for different orders of the Neumann expansion ($P_2 = \{0, 1, 2, 3, 4, 5\}$) when the correlation length is set at $\mu = L/50$.

even value returns an equivalent value for the normalised approximate L^2 relative error of the mean.

In a similar manner the normalised approximate L^2 relative error of the standard deviation of the normalised response vector is also considered

$$\hat{\epsilon}^{\sigma}_{L^2}(\theta) = \frac{\|\boldsymbol{\sigma}_{DMCS}(\theta) - \boldsymbol{\sigma}_{CM}(\theta)\|_{L^2}}{\|\boldsymbol{\sigma}_{DMCS}(\theta)\|_{L^2}} \tag{70}$$

where $\boldsymbol{\sigma}_{DMCS}$ denotes the standard deviation of the response vector obtained by using the benchmark DMCS method and $\boldsymbol{\sigma}_{CM}$ denotes the standard deviation of the response vector obtained by a comparable method. The error measurement has again been explored for different orders of the Neumann and the polynomial chaoses. The normalised approximate L^2 relative error of the standard deviation is depicted in Figs. 8, 9 and 10. Similarly to the case of the normalised approximate L^2 relative error of the mean, six different values for the order of the

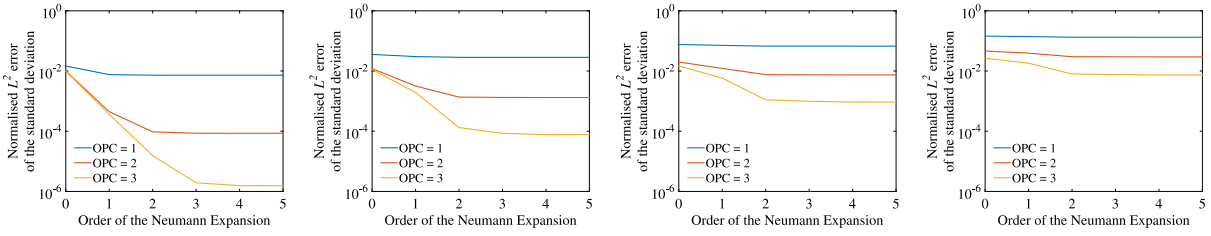

Fig. 8. The normalised approximate L^2 relative error of the standard deviation of the response vector for all values of the standard deviation of the bending rigidity $\sigma_a = \{0.05, 0.10, 0.15, 0.20\}$. The normalised approximate L^2 relative error of the standard deviation of the response vector has been depicted for different orders of the polynomial chaos expansion ($P_1 = \{1, 2, 3\}$) and for different orders of the Neumann expansion ($P_2 = \{0, 1, 2, 3, 4, 5\}$) when the correlation length is set at $\mu = L$.

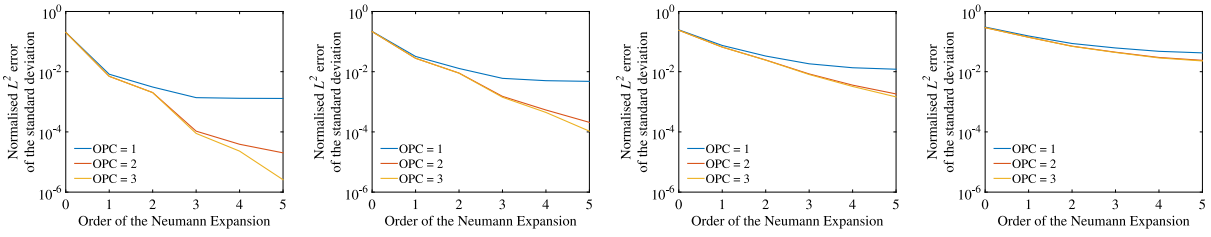

Fig. 9. The normalised approximate L^2 relative error of the standard deviation of the response vector for all values of the standard deviation of the bending rigidity $\sigma_a = \{0.05, 0.10, 0.15, 0.20\}$. The normalised approximate L^2 relative error of the standard deviation of the response vector has been depicted for different orders of the polynomial chaos expansion ($P_1 = \{1, 2, 3\}$) and for different orders of the Neumann expansion ($P_2 = \{0, 1, 2, 3, 4, 5\}$) when the correlation length is set at $\mu = L/25$.

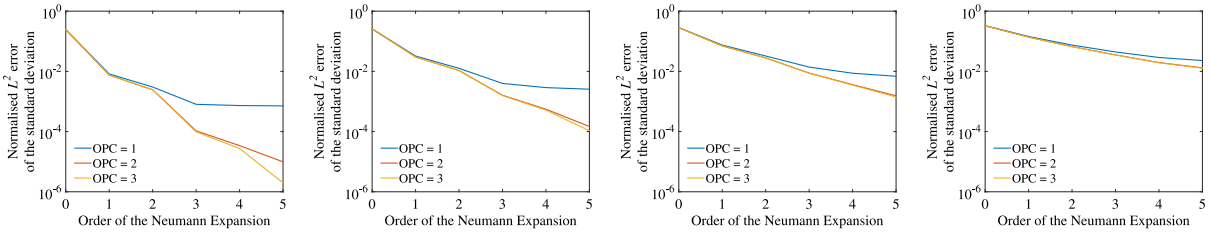

Fig. 10. The normalised approximate L^2 relative error of the standard deviation of the response vector for all values of the standard deviation of the bending rigidity $\sigma_a = \{0.05, 0.10, 0.15, 0.20\}$. The normalised approximate L^2 relative error of the standard deviation of the response vector has been depicted for different orders of the polynomial chaos expansion ($P_1 = \{1, 2, 3\}$) and for different orders of the Neumann expansion ($P_2 = \{0, 1, 2, 3, 4, 5\}$) when the correlation length is set at $\mu = L/50$.

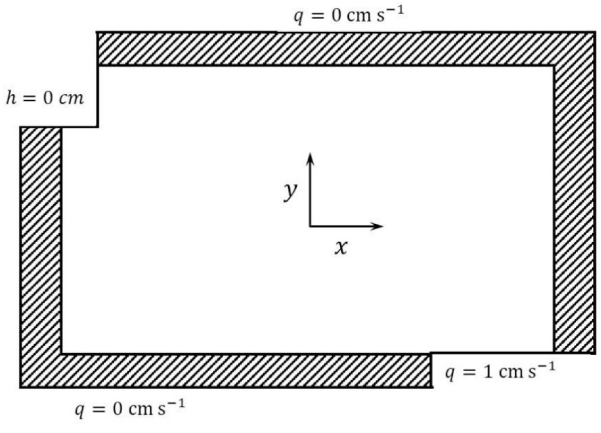

Fig. 11. The configuration of the stochastically parametrised flow system.

Neumann series expansion are given along the x-axis. Three different orders for the polynomial chaoses are explored. "OPC = 1" again corresponds to the first order, "OPC = 2" to the second and "OPC = 3" corresponds to the third.

It can be observed that increasing the order of the polynomial chaos expansion produces a lower quantity of error. However, as the order of the Neumann series expansion increases the reduction in the induced error saturates. The lower the order of the polynomial chaos expansion and the smaller the value of σ_a the earlier the saturation. This is most apparent when the correlation length is set to L. In a similar manner to the normalised approximate L^2 relative error of the mean, the higher the value of σ_a the smaller the difference between the induced errors when altering the order of the polynomial chaoses. As expected, a step-wise pattern is not apparent in the normalised approximate L^2 relative error of the standard deviation. However due to the step-wise nature of the normalised approximate L^2 relative error of the mean, care must be taken in order to choose the optimal order for the Neumann series expansion.

6.2. Flow through a stochastic porous media

In order to scrutinise the proposed method in a higher spatial domain, a two-dimensional domain is examined. This is undertaken by considering a flow through a two-dimensional porous media, where it is

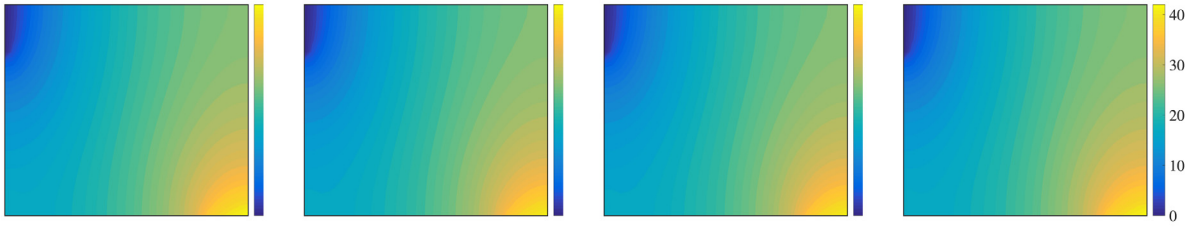

Fig. 12. Contour plots of the mean of the head (cm) obtained by using the DMCS, PC, NEPC1 and NEPC2 methods. The x and y axis are respectively the positions in the x direction with $x \in [-0.25, 0.25]$ and y in the direction with $y \in [-0.15, 0.15]$.

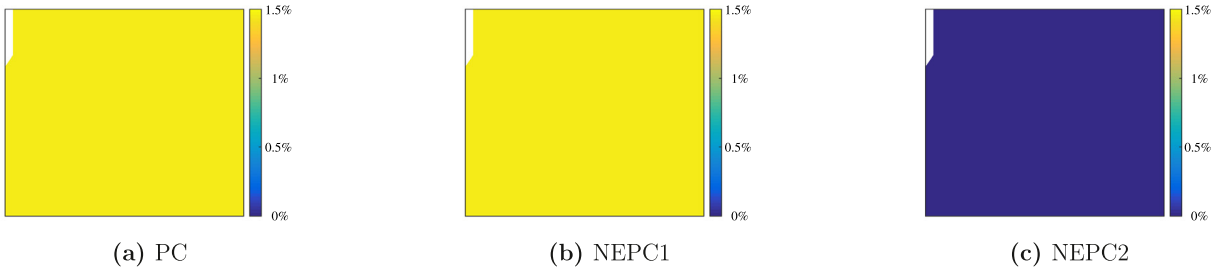

Fig. 13. Contour plots of the percentage error arising in the mean of the head (cm) when utilising the PC, NEPC1 and NEPC2 methods in comparison to the DMCS method. The x and y axis are respectively the positions in the x direction with $x \in [-0.25, 0.25]$ and y in the direction with $y \in [-0.15, 0.15]$.

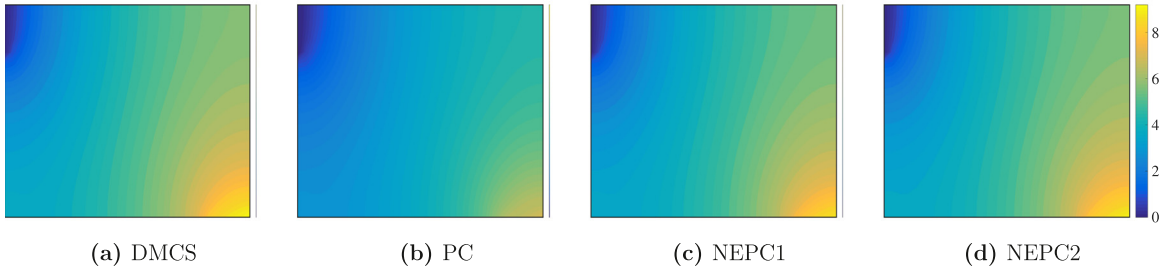

Fig. 14. Contour plots of the standard deviation of the head (cm) obtained by using the DMCS, PC, NEPC1 and NEPC2 methods. The x and y axis are respectively the positions in the x direction with $x \in [-0.25, 0.25]$ and y in the direction with $y \in [-0.15, 0.15]$.

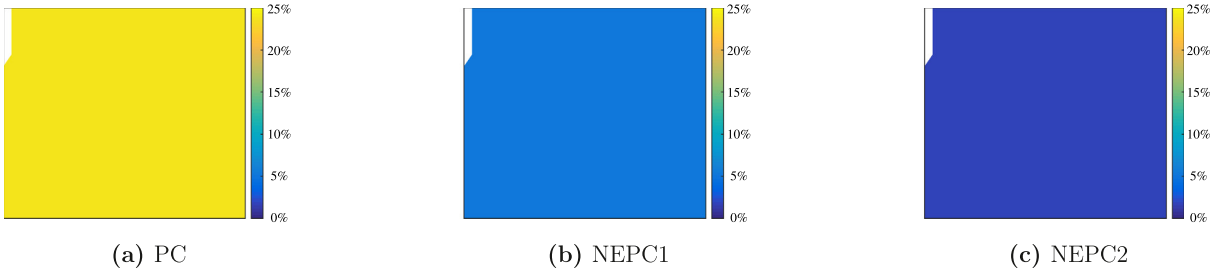

Fig. 15. Contour plots of the percentage error arising in the standard deviation of the head (cm) when utilising the PC, NEPC1 and NEPC2 methods in comparison to the DMCS method. The x and y axis are respectively the positions in the x direction with $x \in [-0.25, 0.25]$ and y in the direction with $y \in [-0.15, 0.15]$.

assumed that the porous media contains stochastic properties. The two-dimensional domain under consideration is a rectangle of length $L = 0.50$ m and height $H = 0.30$ m. This is illustrated by Fig. 11. Through the use of the stochastic finite element method, the rectangular domain is represented by an uniform 30×18 mesh containing 540 square elements. The centre of the domain is represented by the coordinate (0.00, 0.00). Our measurement of interest is head of the system. This quantity is subsequently computed at each of the nodes of the domain. The head, h, is fixed to 0.00 cm along $x = -0.25$ m, $y = [0.08, 0.15]$ m. This ensures that the system reaches a steady state. A constant flux $q = 1.00$ cm s^{-1} is applied along $x = [0.12, 0.15]$ m, $y = -0.15$ m. The flux is zero along the remaining boundary i.e. $q = 0.00$ cm s^{-1}. To take account of the stochasticity of the system, a Gaussian hydraulic conductivity (k) which has a two-dimensional autocovariance kernel is considered. To obtain the two-dimensional autocovariance kernel, two one-dimensional exponential autocovariance kernels are considered. The first one-dimensional exponential autocovariance kernel depends on x and has a correlation length of $\frac{3L}{2}$ whilst the second depends on y and has a correlation length of $\frac{3H}{2}$. To obtain the two-dimensional autocovariance kernel, the product of both the one-dimensional exponential autocovariance kernels are taken. In both the one-dimensional

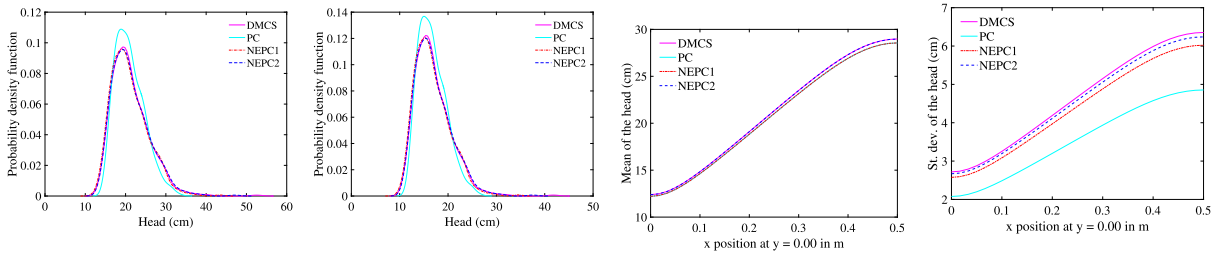

(a) Probability density function at $(0.00, 0.00)$

(b) Probability density function at $(-0.15, 0.08)$

(c) Mean of the head along $y = 0.00$ m

(d) Standard deviation of the head along $y = 0.00$ m

Fig. 16. The probability density function of the head (cm) computed by the DMCS, PC, NEPC1 and NEPC2 methods at $(0.00, 0.00)$ and $(-0.15, 0.08)$ as well as the mean and standard deviation of the head along $y = 0.00$ m.

exponential autocovariance kernels, 8 terms have been retained in the Karhunen–Loève expansions. This results in the full Karhunen–Loève expansion containing 64 terms in addition to the deterministic matrix $\mathbf{A}_0$. The mean of the hydraulic conductivity is set as $\bar{k} = 1$ cm s^{-1}. The value of the input standard deviation is set as: $\sigma_a = \{0.15\}$. For all the considered methods 5,000 samples have been observed. 5,000 samples ensures the convergence of the first two moments of interest. For the PC method 4 terms from the Karhunen–Loève expansions have been considered. Thus the enriched NEPC method incorporates an additional 60 terms from the Karhunen–Loève expansions. Both methods have utilised second order polynomial chaoses. If the PC method were to incorporate 64 terms from the Karhunen–Loève expansions, a linear system of size $1,252,680 \times 1,252,680$ would require solving.

Fig. 12 illustrates the mean of the head for the four methods under examination. To further examine the effectiveness of the approximation methods in capturing the mean DMCS method, the percentage error of the mean of the head is illustrated in Fig. 13. The percentage error of the mean is represented by

$$\bar{\varepsilon}_{\%} = 100 \times \frac{|\text{mDMCS} - \text{mCOMP}|}{\text{mDMCS}} \tag{71}$$

where mDMCS corresponds to the mean of the DMCS method and mCOMP corresponds to the mean of a comparable method. It is apparent from Fig. 13 that both the PC and NEPC1 methods induce the same quantity of error. When a second order Neumann expansion is utilised within the Neumann Enriched Polynomial Chaos method i.e. NEPC2, a visible reduction in the error is noticeable. In a similar manner, the standard deviation of the head is illustrated in Fig. 14 for all four methods. Contrary to the mean of the head, a visible and evident difference is seen between the approximation methods. To further illustrate the differences, the percentage error of the standard deviation, $\tilde{\varepsilon}_{\%}$, is considered

$$\tilde{\varepsilon}_{\%} = 100 \times \frac{|\text{sDMCS} - \text{sCOMP}|}{\text{sDMCS}} \tag{72}$$

where sDMCS corresponds to the standard deviation of the DMCS method and sCOMP corresponds to the standard deviation of a comparable method. The contour plots of the percentage error are depicted in Fig. 15. By increasing the order of the Neumann expansion method contained within the Neumann Enriched Polynomial Chaos method the percentage error visibly decreases. This is in agreement with the discussion held in Section 5. The probability density function of the head of the system is illustrated for two different locations in the spatial domain in Fig. 16. These locations possess the following coordinates: $(0.00, 0.00)$ and $(-0.15, 0.08)$. The probability density functions further enhances the accuracy improvement obtained following the implementation of the Neumann Enriched Polynomial Chaos method. Fig. 16 also illustrates the mean and standard deviation of the head along all nodes of the structure when $y = 0.00$ m.

7. Summary and conclusion

This paper brings together two very different uncertainty propagation approaches, namely the polynomial chaos and Neumann expansion. These methods have been historically viewed as incompatible as polynomial chaos is a 'global representation' while the Neumann expansion is a 'local representation'. A novel polynomial chaos enrichment method has been proposed to approximate the response of stochastically parametrised systems. The proposed method is initiated by partitioning the random variables associated with the stochastic finite element method into two sets. Based on a first-order sensitivity analysis, *relative importance factors* have been introduced to rationally partition the stochastic space into two sets. A low-ordered polynomial chaos expansion is executed on the first set whilst the second set is utilised to enrich the deterministic vectors associated with the polynomial chaos expansion [PCE]. The enrichment is based upon a Neumann series expansion. The enrichment method results in the following seemingly minor modification to the unknown vectors associated with the classical PCE method

$$\mathbf{U}_y(\theta) \approx \left[\mathbf{I} + \underbrace{\sum_{k=1}^{P_2} \left(-\widetilde{\mathbf{A}}_0^{-1} \sum_{j=1}^{M_2} y_j(\theta) \widetilde{\mathbf{B}}_j \right)^k}_{\text{the contribution of the enrichment method}} \right] \mathbf{U}_0 \tag{73}$$

where the additional contribution associated with the enrichment method is computed by utilising a Neumann series expansion of order P_2. The enrichment method ensures that a large number of random variables can be utilised in conjunction with the PCE framework. Exact closed-form expressions have been developed to obtain the first two statistical moments of the response vector. The primary advantages of the proposed method include:

- The ability to tailor computational cost and accuracy by suitably partitioning the space of random variables, selecting the order of the polynomial chaos and selecting the order of the Neumann expansion.
- The traditional polynomial chaos approach appears as a special case when the space of random variables is not partitioned.
- Should a truncated set of variables be used in a polynomial chaos expansion; the approach provides an explicit quantification of the impact of the ignored random variables on the response statistics.

The Neumann enriched polynomial chaos method has been applied to analyse the bending of an Euler–Bernoulli cantilever beam and the head of a flow through a porous media. The results have been compared with the classical polynomial chaos expansion method and the direct Monte Carlo method. It is apparent that utilising the enrichment method can significantly reduce the error in comparison to the PCE method with original random variables. It has been proven and demonstrated that employing the enrichment method with a Neumann

series of an even valued order is required to ensure a reduction in the induced error of the first two moments of the response. Further research is needed to determine the optimal order and the optimal number of random variables associated with both the polynomial chaos and Neumann series expansions. The case when the basic input variables appear as nonlinear functions should be considered in future research.

Declaration of competing interest

The authors declare that they have no known competing financial interests or personal relationships that could have appeared to influence the work reported in this paper.

Acknowledgements

The authors acknowledge the financial support received from Engineering Research Network Wales, UK (one of three Sêr Cymru National Research Networks) through the award of NRN125 grant.

References

[1] N. Wiener, The homogeneous chaos, Amer. J. Math. 60 (4) (1938) 897–936.
[2] R.G. Ghanem, P.D. Spanos, Stochastic Finite Elements: A Spectral Approach, revised ed., Dover Publications Inc., 2012.
[3] A. Sarkar, R. Ghanem, Mid-frequency structural dynamics with parameter uncertainty, Comput. Methods Appl. Mech. Engrg. 191 (47–48) (2002) 5499–5513.
[4] E. Jacquelin, S. Adhikari, J.-J. Sinou, M. Friswell, Polynomial chaos expansion in structural dynamics: Accelerating the convergence of the first two statistical moment sequences, J. Sound Vib. 356 (2015) 144–154.
[5] L. Codecasa, L. Di Rienzo, Stochastic thermal modeling by polynomial chaos expansion, in: 19th International Workshop on Thermal Investigations of ICs and Systems, THERMINIC, IEEE, 2013, pp. 33–38.
[6] V.A.B. Narayanan, N. Zabaras, Stochastic inverse heat conduction using a spectral approach, Internat. J. Numer. Methods Engrg. 60 (9) (2004) 1569–1593.
[7] H.N. Najm, Uncertainty quantification and polynomial chaos techniques in computational fluid dynamics, Annu. Rev. Fluid Mech. 41 (1) (2009) 35–52.
[8] O.M. Knio, O.P. Le Maître, Uncertainty propagation in CFD using polynomial chaos decomposition, Fluid Dyn. Res. 38 (9) (2006) 616–640.
[9] B. Pascual, S. Adhikari, A reduced polynomial chaos expansion method for the stochastic finite element analysis, Sadhana 37 (3) (2012) 319–340.
[10] H.C. Ozen, G. Bal, A dynamical polynomial chaos approach for long-time evolution of SPDEs, J. Comput. Phys. 343 (2017) 300–323.
[11] E. Jacquelin, S. Adhikari, J.-J. Sinou, M.I. Friswell, Polynomial chaos expansion and steady-state response of a class of random dynamical systems, J. Eng. Mech. 141 (4) (2015) 04014145.
[12] V. Yaghoubi, S. Marelli, B. Sudret, T. Abrahamsson, Sparse polynomial chaos expansions of frequency response functions using stochastic frequency transformation, Probab. Eng. Mech. 48 (2017) 39–58.
[13] R. Ghanem, D. Ghosh, Efficient characterization of the random eigenvalue problem in a polynomial chaos decomposition, Internat. J. Numer. Methods Engrg. 72 (4) (2007) 486–504.
[14] D. Ghosh, R. Ghanem, Stochastic convergence acceleration through basis enrichment of polynomial chaos expansions, Internat. J. Numer. Methods Engrg. 73 (2) (2008) 162–184.
[15] B. Pascual, S. Adhikari, Hybrid perturbation-polynomial chaos approaches to the random algebraic eigenvalue problem, Comput. Methods Appl. Mech. Engrg. 217–220 (2012) 153–167.
[16] M. Herzog, A. Gilg, M. Paffrath, P. Rentrop, U. Wever, Intrusive versus non-intrusive methods for stochastic finite elements, in: From Nano to Space, Springer Berlin Heidelberg, Berlin, Heidelberg, 2008, pp. 161–174.
[17] O.P. Le Maître, M.T. Reagan, H.N. Najm, R.G. Ghanem, O.M. Knio, A stochastic projection method for fluid flow: II. Random process, J. Comput. Phys. 181 (1) (2002) 9–44.
[18] D.M. Ghiocel, R.G. Ghanem, Stochastic finite-element analysis of seismic soil–structure interaction, J. Eng. Mech. 128 (1) (2002) 66–77.
[19] Z. Gao, T. Zhou, On the choice of design points for least square polynomial approximations with application to uncertainty quantification, Commun. Comput. Phys. 16 (02) (2014) 365–381.
[20] J. Hampton, A. Doostan, Coherence motivated sampling and convergence analysis of least squares polynomial Chaos regression, Comput. Methods Appl. Mech. Engrg. 290 (2015) 73–97.
[21] B. Ganis, H. Klie, M.F. Wheeler, T. Wildey, I. Yotov, D. Zhang, Stochastic collocation and mixed finite elements for flow in porous media, Comput. Methods Appl. Mech. Engrg. 197 (43–44) (2008) 3547–3559.
[22] I. Babuška, F. Nobile, R. Tempone, A stochastic collocation method for elliptic partial differential equations with random input data, SIAM J. Numer. Anal. 45 (3) (2007) 1005–1034.
[23] G. Blatman, B. Sudret, M. Berveiller, Quasi random numbers in stochastic finite element analysis, Méc. Ind. 8 (3) (2007) 289–297.
[24] S.-K. Choi, R.V. Grandhi, R.A. Canfield, C.L. Pettit, Polynomial chaos expansion with latin hypercube sampling for estimating response variability, AIAA J. 42 (6) (2004) 1191–1198.
[25] M. Eldred, J. Burkardt, Comparison of non-intrusive polynomial chaos and stochastic collocation methods for uncertainty quantification, in: 47th AIAA Aerospace Sciences Meeting Including the New Horizons Forum and Aerospace Exposition, American Institute of Aeronautics and Astronautics, Reston, Virigina, 2009.
[26] M. Hadigol, A. Doostan, Least squares polynomial chaos expansion: A review of sampling strategies, Comput. Methods Appl. Mech. Engrg. 332 (2018) 382–407.
[27] S. Hosder, R. Walters, Non-intrusive polynomial chaos methods for uncertainty quantification in fluid dynamics, in: 48th AIAA Aerospace Sciences Meeting Including the New Horizons Forum and Aerospace Exposition, American Institute of Aeronautics and Astronautics, Reston, Virigina, 2010.
[28] S. Hosder, R. Walters, M. Balch, Efficient sampling for non-intrusive polynomial chaos applications with multiple uncertain input variables, in: 48th AIAA/ASME/ASCE/AHS/ASC Structures, Structural Dynamics, and Materials Conference, American Institute of Aeronautics and Astronautics, Reston, Virigina, 2007.
[29] K. Cheng, Z. Lu, Adaptive sparse polynomial chaos expansions for global sensitivity analysis based on support vector regression, Comput. Struct. 194 (2018) 86–96.
[30] S. Abraham, M. Raisee, G. Ghorbaniasl, F. Contino, C. Lacor, A robust and efficient stepwise regression method for building sparse polynomial chaos expansions, J. Comput. Phys. 332 (2017) 461–474.
[31] J. Peng, J. Hampton, A. Doostan, A weighted L1-minimization approach for sparse polynomial chaos expansions, J. Comput. Phys. 267 (2014) 92–111.
[32] C. Hu, B.D. Youn, Adaptive-sparse polynomial chaos expansion for reliability analysis and design of complex engineering systems, Struct. Multidiscip. Optim. 43 (3) (2011) 419–442.
[33] G. Blatman, B. Sudret, Adaptive sparse polynomial chaos expansion based on least angle regression, J. Comput. Phys. 230 (6) (2011) 2345–2367.
[34] E. Pagnacco, E. Sarrouy, R. Sampaio, E. Souza de Cursi, Pitfalls in the frequency response represented onto polynomial chaos for random SDOF mechanical systems, Appl. Math. Model. 52 (2017) 626–647.
[35] F. Augustin, A. Gilg, M. Paffrath, P. Rentrop, U. Wever, Polynomial chaos for the approximation of uncertainties: Chances and limits, European J. Appl. Math. 19 (02) (2008) 149–190.
[36] B.J. Debusschere, H.N. Najm, P.P. Pébay, O.M. Knio, R.G. Ghanem, O.P. Le Maître, Numerical challenges in the use of polynomial chaos representations for stochastic processes, SIAM J. Sci. Comput. 26 (2) (2004) 698–719.
[37] F.T. Wong, W. Kanok-Nukulchai, On the convergence of the kriging-based finite element method, Int. J. Comput. Methods 06 (01) (2009) 93–118.
[38] R. Schöbi, B. Sudret, S. Marelli, Rare event estimation using polynomial-chaos kriging, ASCE-ASME J. Risk Uncertain. Eng. Syst. A 3 (2) (2017) D4016002.
[39] R. Schöbi, B. Sudret, J. Wiart, Polynomial-chaos-based kriging, Int. J. Uncertain. Quantif. 5 (2015) 171–193.
[40] Z. Bai, Krylov subspace techniques for reduced-order modeling of large-scale dynamical systems, Appl. Numer. Math. 43 (1–2) (2002) 9–44.
[41] J. Yang, B. Faverjon, H. Peters, N. Kessissoglou, Application of polynomial chaos expansion and model order reduction for dynamic analysis of structures with uncertainties, Procedia IUTAM 13 (2015) 63–70.
[42] D.B. Xiu, G.E. Karniadakis, The wiener-askey polynomial chaos for stochastic differential equations, SIAM J. Sci. Comput. 24 (2) (2002) 619–644.
[43] D.B. Xiu, G.E. Karniadakis, Modeling uncertainty in flow simulations via generalized polynomial chaos, J. Comput. Phys. 187 (1) (2003) 137–167.
[44] A. Papoulis, S.U. Pillai, Probability, Random Variables, and Stochastic Processes, McGraw-Hill, 2002.